Mo–total organic carbon covariation in modern anoxic marine environments: Implications for analysis of paleoredox and paleohydrographic conditions

Thomas J. Algeo[1] and Timothy W. Lyons[2]

Received 5 November 2004; revised 12 September 2005; accepted 21 December 2005; published 28 March 2006.

[1] Sedimentary molybdenum, $[Mo]_s$, has been widely used as a proxy for benthic redox potential owing to its generally strong enrichment in organic-rich marine facies deposited under oxygen-depleted conditions. A detailed analysis of $[Mo]_s$–total organic carbon (TOC) covariation in modern anoxic marine environments and its relationship to ambient water chemistry suggests that (1) $[Mo]_s$, while useful in distinguishing oxic from anoxic facies, is not related in a simple manner to dissolved sulfide concentrations within euxinic environments and (2) patterns of $[Mo]_s$-TOC covariation can provide information about paleohydrographic conditions, especially the degree of restriction of the subchemoclinal water mass and temporal changes thereof related to deepwater renewal. These inferences are based on data from four anoxic silled basins (the Black Sea, Framvaren Fjord, Cariaco Basin, and Saanich Inlet) and one upwelling zone (the Namibian Shelf), representing a spectrum of aqueous chemical conditions related to water mass restriction. In the silled-basin environments, increasing restriction is correlated with a systematic decrease in $[Mo]_s$/TOC ratios, from $\sim$45 ± 5 for Saanich Inlet to $\sim$4.5 ± 1 for the Black Sea. This variation reflects control of $[Mo]_s$ by $[Mo]_{aq}$, which becomes depleted in stagnant basins through removal to the sediment without adequate resupply by deepwater renewal (the ''basin reservoir effect''). The temporal dynamics of this process are revealed by high-resolution chemostratigraphic data from Framvaren Fjord and Cariaco Basin sediment cores, which exhibit long-term trends toward lower $[Mo]_s$/TOC ratios following development of water column stratification and deepwater anoxia. Mo burial fluxes peak in weakly sulfidic environments such as Saanich Inlet (owing to a combination of greater $[Mo]_{aq}$ availability and enhanced Mo transport to the sediment-water interface via Fe-Mn redox cycling) and are lower in strongly sulfidic environments such as the Black Sea and Framvaren Fjord. These observations demonstrate that, at timescales associated with deepwater renewal in anoxic silled basins, decreased sedimentary Mo concentrations and burial fluxes are associated with lower benthic redox potentials (i.e., more sulfidic conditions). These conclusions apply only to anoxic marine environments exhibiting some degree of water mass restriction (e.g., silled basins) and are not valid for low-oxygen facies in open marine settings such as continent-margin upwelling systems.

Citation: Algeo, T. J., and T. W. Lyons (2006), Mo–total organic carbon covariation in modern anoxic marine environments: Implications for analysis of paleoredox and paleohydrographic conditions, *Paleoceanography*, *21*, PA1016, doi:10.1029/2004PA001112.

1. Introduction

[2] Molybdenum (Mo) is the most abundant transition element in the modern ocean, with a concentration of $\sim$105 ± 5 nmol kg^{-1} and a residence time of $\sim$800 kyr [*Wright and Colling*, 1995; *Millero*, 1996]. Its abundance and long residence time in seawater are due to its conservative behavior under oxic conditions, which favor formation of the stable and largely unreactive molybdate oxyanion (MoO_4^{2-}). Under anoxic conditions, Mo is readily transferred to the sediment by adsorption onto humic substances and Mn-oxyhydroxides or by uptake in solid solution with authigenic Fe-sulfides [*Berrang and Grill*, 1974; *Magyar et al.*, 1993; *Morse and Luther*, 1999; *Adelson et al.*, 2001], possibly facilitated by the formation of particle-reactive thiomolybdates [*Helz et al.*, 1996; *Erickson and Helz*, 2000; *Vorlicek and Helz*, 2002]. Although oxic-suboxic facies are the most important sink for seawater Mo in the modern ocean, its burial flux is considerably greater under reducing conditions, as shown by the fact that anoxic facies account for $\sim$30–50% of the global Mo sink at present despite making up only $\sim$0.3% of total seafloor area [*Bertine and Turekian*, 1973; *Morford and Emerson*, 1999; *Anbar*, 2004]. Larger areas of anoxic marine sedimentation in the past may have resulted in substantially greater Mo burial fluxes, with implications for nitrogen fixation and the evolution of marine ecosys-

[1]Department of Geology, University of Cincinnati, Cincinnati, Ohio, USA.
[2]Department of Earth Sciences, University of California, Riverside, California, USA.

0883-8305/06/2004PA001112$12.00

tems [*Anbar and Knoll*, 2002; *Arnold et al.*, 2004; *Algeo*, 2004].

[3] Sedimentary Mo has been widely used in paleoceanographic studies as a redox proxy [e.g., *Emerson and Huested*, 1991; *Jones and Manning*, 1994; *Crusius et al.*, 1999; *Morford et al.*, 2001; *Piper and Dean*, 2002; *Algeo et al.*, 2004], a practice based on general patterns of trace element enrichment in modern anoxic marine environments and ancient black shales [e.g., *Calvert and Price*, 1970; *Hirst*, 1974; *Holland*, 1984]. Although sedimentary Mo enrichment is indisputably associated with the transition from oxic to anoxic-sulfidic conditions on the seafloor, a systematic relationship between benthic redox variation and $[Mo]_s$ has not been demonstrated within euxinic environments. Yet such a relationship (i.e., higher $[Mo]_s$ under more sulfidic conditions) might be inferred on the basis of (1) the broad redox dependency of sedimentary Mo accumulation (i.e., in oxic versus anoxic facies), and (2) the kinetics of molybdate sulfidation in intermittently euxinic facies (i.e., longer exposure to critical concentrations of aqueous H_2S required for formation of the more particle-reactive higher thiomolybdates [*Erickson and Helz*, 2000]). Determining whether such a relationship exists is essential if sedimentary Mo is to serve as more than a general indicator of paleoredox conditions. In the present study, analysis of aqueous and sedimentary geochemical data from five modern anoxic marine systems (i.e., the Black Sea, Framvaren Fjord, Cariaco Basin, Saanich Inlet, and Namibian Shelf) revealed that sedimentary Mo concentrations, rather than increasing at lower benthic redox potentials, generally decrease as bottom waters become more sulfidic. This "counterintuitive" relationship suggests that our understanding of controls on sedimentary Mo accumulation in anoxic facies is incomplete, and that some reassessment of the sensitivity of sedimentary Mo as a paleoredox proxy is necessary.

[4] A potentially important control on sedimentary Mo that has received scant attention to date is the availability of aqueous Mo in anoxic marine systems. In environments with restricted deepwater exchange (e.g., silled basins), aqueous Mo concentrations can become substantially depleted through removal to the sediment without adequate resupply, e.g., Black Sea deep waters contain only 3–5% as much Mo as seawater (on a salinity-normalized basis). Reduced availability of aqueous Mo may leave a signature in the trace metal chemistry of organic-rich sediments, in which most Mo is of hydrogenous origin. The modern anoxic marine environments examined in this study are useful in examining this issue because they include four silled basins exhibiting a spectrum of degrees of deepwater restriction from weak (Saanich Inlet) to strong (the Black Sea) and one continent-margin upwelling system that is not subject to deepwater restriction (the Namibian Shelf) as a "control." Although other factors almost certainly play a role, geographic and stratigraphic variation in sediment Mo/TOC ratios in these environments can be linked to spatial and temporal changes in water mass chemistry that, in some instances, can be associated with known historical or geological events affecting basin hydrography. The present analysis demonstrates that sedimentary Mo-TOC relationships have considerable, as yet unrealized potential as an indicator of hydrographic conditions in anoxic paleoenvironments.

[5] The results of the present study also have significant implications for several other issues pertaining to anoxic marine systems. First, there is uncertainty regarding the dominant vectors of Mo transfer to the sediment. Aqueous and sedimentary geochemical relationships documented in this study place significant constraints on the relative importance of various host phases (e.g., organic matter, Fe-sulfides, and Fe-Mn-oxyhydroxides) as well as on the locus of Mo uptake (e.g., in the water column, at the sediment-water interface, or within the sediment) in the investigated environments. Second, existing classifications of anoxic marine environments consist of discrete models based on conceptualized geographic and hydrographic conditions ("silled basins," "upwelling systems," etc.) [e.g., *Demaison and Moore*, 1980; *Arthur and Sageman*, 1994; *Wignall*, 1994]. A new approach to evaluation of anoxic paleoenvironments would utilize environmental parameters that can be estimated from measurable, objective criteria. For example, the degree of restriction of the subpycnoclinal water mass, which varies in modern marine environments over a continuum from highly restricted silled basins (e.g., Black Sea) to weakly restricted silled basins (e.g., Saanich Inlet) and unrestricted continent-margin upwelling systems (e.g., Namibian Shelf), can be estimated in paleoenvironments on the basis of sedimentary Mo-TOC relationships.

2. Modern Anoxic Marine Environments

[6] More than a score of Recent anoxic marine and marginal marine environments have been studied to at least a limited degree; the five environments examined in this study were selected on the basis of availability of published aqueous and sedimentary Mo geochemical data. The Black Sea, Framvaren Fjord, Cariaco Basin, and Saanich Inlet are generally classified as silled basins, in which an oxygenated surface water layer is separated from a sulfidic deepwater layer by a chemocline (i.e., O_2-H_2S interface) that is roughly coextant with a major pycnocline (i.e., density gradient) within the water column. The Namibian Shelf represents a continent-margin upwelling zone; such systems lack topographic barriers to water mass circulation and, consequently, exhibit highly dynamic aqueous chemical conditions. These five anoxic systems display markedly different boundary conditions: (1) Physically, they vary in volume from 3.3 km^3 for Framvaren Fjord to 541,000 km^3 for the Black Sea; (2) tectonically, they represent diverse settings including stable craton (Framvaren Fjord), passive margin (Namibian Shelf), uplifted convergent margin (Saanich Inlet), subducted convergent margin (Cariaco Basin), and intracontinental ocean basin (Black Sea); and (3) climatically, they represent the humid tropical (Cariaco), arid subtropical (Black Sea, Namibian Shelf), temperate (Saanich Inlet), and boreal (Framvaren Fjord) zones. Despite such differences, these five anoxic marine systems exhibit a continuum with respect to hydrographic conditions, as reflected in the aqueous chemistry

Table 1. Geographic and Hydrographic Parameters of Modern Anoxic Marine Environments

	Volume, km^3	Sill Depth, m	Chemocline Depth, m	Total Depth, m	Sill Depth/Total Depth	Chemocline Depth/Total Depth	Deepwater Age, τ_{dw}, years
Black Sea[a]	541,000	33	50–150	2240	0.015	0.02–0.06	500–4,000
Framvaren Fjord[b]	0.33	2	18–20	183	0.011	0.10–0.11	50–130 (1600?)
Cariaco Basin[c]	8,000	146	250–375	1425	0.10	0.18–0.26	50–100
Saanich Inlet[d]	5.4	70	150–238	238	0.29	0.63–1.0	~1.5
Namibian Shelf[e]	~1000	none	none	0–200	1.0	1.0	~0

[a] *Brewer and Spencer* [1974], *Gunnerson and Özturgut* [1974], *Murray* [1991a], *Murray et al.* [1991], and *Dyrssen et al.* [1996].
[b] *Skei* [1981, 1983, 1986], *Jacobs* [1984], *Dyrssen et al.* [1996], and *Dyrssen* [1999].
[c] *Deuser* [1973], *Jacobs* [1984], *Scranton et al.* [1987, 2001], and *Piper and Dean* [2002].
[d] *Jacobs* [1984], *François* [1987] and *Shipboard Scientific Party* [1998].
[e] *Price and Calvert* [1973], *Chapman and Bailey* [1991], and *Dingle and Nelson* [1993].

and degree of restriction of their subpycnoclinal water masses.

2.1. Physical Setting and Geologic Background

2.1.1. Black Sea

[7] The Black Sea, the largest modern anoxic marine system, is a 423,000-km^2 restricted ocean basin with a maximum depth of 2240 m and a sill depth of 33 m in the Bosporus Strait (Table 1 and Figures 1a and 2a) [*Gunnerson and Özturgut*, 1974; *Murray*, 1991a]. It has a large (2.2×10^6 km^2) drainage basin with strong runoff (11,800–12,600 m^3 s^{-1}), resulting in a positive water balance and estuarine-type circulation. The chemocline is presently at ~50-m water depth in the basin center and ~120–150 m around the basin margins (Figure 2a), although its position has fluctuated in both the premodern and modern periods [*Brewer and Spencer*, 1974; *Murray et al.*, 1989; *Tugrul et al.*, 1992; *Lyons et al.*, 1993; *Anderson et al.*, 1994; *Wilkin and Arthur*, 2001]. The recent ~50-m rise in the chemocline has been linked to changes in water mass salinity and temperature; on a density-normalized basis, the chemocline has been relatively stable. The Black Sea was a freshwater lake until the postglacial rise in sea level caused marine waters to transgress the Bosporus sill at ~7540 years B.P. [*Jones and Gagnon*, 1994; *Wilkin et al.*, 1997]. The modern Black Sea exhibits variable but generally low rates of organic carbon (~1–10 g m^{-2} yr^{-1}) and bulk sediment accumulation (10–200 g m^{-2} yr^{-1}), both increasing toward the basin margins (Table 2) [*Shimkus and Trimonis*, 1974; *Calvert et al.*, 1991; *Karl and Knauer*, 1991; *Arthur et al.*, 1994].

2.1.2. Framvaren Fjord

[8] Framvaren is a 5.8-km^2 fjord in southern Norway with a maximum depth of 183 m and a sill depth of 2.5 m (Table 1 and Figures 1b and 2b) [*Skei*, 1981, 1983, 1986]. It has a small (31 km^2), low-relief drainage basin with modest runoff (1.3 m^3 s^{-1}) and minimal human influence (~100 inhabitants). Framvaren exhibits estuarine-type circulation, although influx of seawater is limited by a long (500 m), shallow (2–2.5 m) sill connecting it to Helvikfjord, Lyngdalsfjord, and ultimately to the open ocean (Figure 1b). Exchange of surface waters with Helvikfjord, which is driven by weak tides and baroclines, occurs at a mean rate of 10 m^3 s^{-1} [*Stigebrandt and Molvaer*, 1988]. The water column is stably stratified with a chemocline at a depth of ~18 m; $[H_2S]_{aq}$ rises rapidly below ~80–100 m owing to the existence of a secondary pycnocline at that level (Figure 2b). Framvaren was an oxic fjord until ~8000 years B.P. when postglacial isostatic rebound converted it to a meromictic lake with sulfidic waters below ~100 m water depth. Dredging of the sill in ~1853 A.D. reconnected Framvaren to the sea and caused the chemocline to rise to the present 18-m level [*Skei*, 1983, 1986]. Rates of bulk sediment (50–120 g m^{-2} yr^{-1}) and organic carbon accumulation (12–24 g m^{-2} yr^{-1}) are moderate (Table 2), and the organic matter is mostly of terrigenous origin [*Skei*, 1981, 1983; *Naes et al.*, 1988; *Dyrssen et al.*, 1996].

2.1.3. Cariaco Basin

[9] The Cariaco Basin, the second largest modern anoxic marine system, is a ~7000-km^2 tectonic depression on the

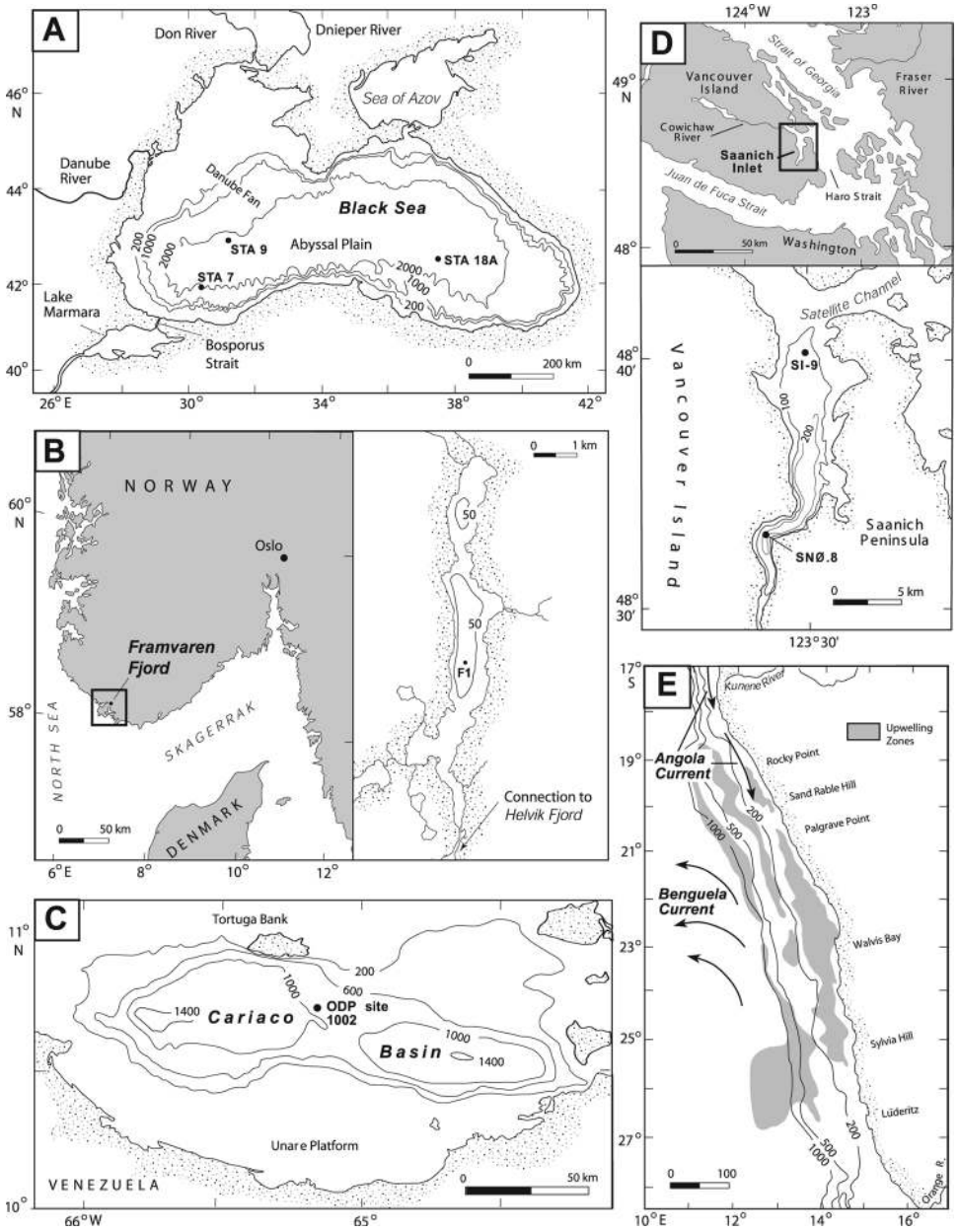

Figure 1. Geography of modern anoxic marine environments: (a) Black Sea, (b) Framvaren Fjord, (c) Cariaco Basin, (d) Saanich Inlet, and (e) Namibian Shelf. Contours are in meters; 50-m contour for Framvaren Fjord is approximate. Locations of gravity and drill cores are shown in Figures 1a–1d. Figure 1a is modified from *Degens and Ross* [1974]; Figure 1b is modified from *Dyrssen* [1999]; Figure 1c is modified from *Piper and Dean* [2002]; Figure 1d is modified from *Jacobs* [1984]; and Figure 1e is modified from *Bremner* [1983].

Venezuelan continental shelf (Figure 1c). The basin, which consists of two >1400-m-deep subbasins separated by a ~900-m-deep saddle, is bordered by a series of shallow sills, principally a 146-m-deep sill on its western margin and a 120-m-deep sill on its northern margin (Table 1 and Figure 1c). These sills limit deepwater exchange, and sulfidic conditions exist below a chemocline that has fluctuated between ~250 and 375 m water depth (Figure 2c) [*Jacobs*, 1984; *Jacobs et al.*, 1987; *Scranton et al.*, 1987, 2001; *Zhang and Millero*, 1993]. Basin waters are fully marine, and water column stratification is maintained by a thermocline. The basin has been intermittently anoxic since at least 580 ka [*Peterson et al.*, 1991, 2000; *Haug et al.*, 1998; *Yarincik et al.*, 2000]. Benthic redox conditions are dependent on sea level elevation, which controls the relative fluxes of surface and intermediate waters from

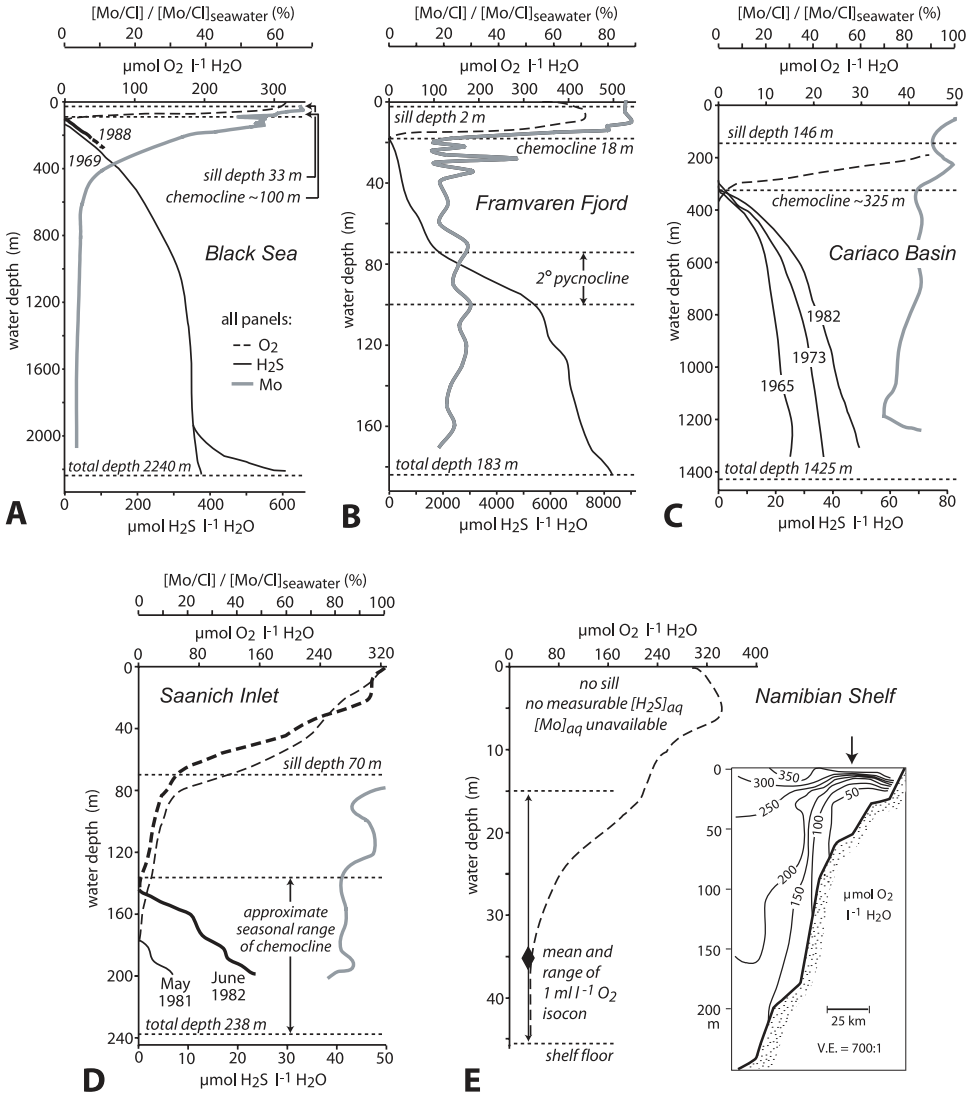

Figure 2. Dissolved O_2, H_2S, and $[Mo]_{aq}$* profiles for modern anoxic marine environments: (a) Black Sea, (b) Framvaren Fjord, (c) Cariaco Basin, (d) Saanich Inlet, and (e) Namibian Shelf (note that the asterisk indicates normalization to seawater salinity). Inset in Figure 2e shows Namibian Shelf dissolved O_2 cross section; arrow indicates position of profile at left (note that data are from St. Helena Bay area, ~500 km southeast of Walvis Bay). Data for Figure 2a are from *Brewer and Spencer* [1974] and *Murray et al.* [1989]; data for Figure 2b are from *Skei* [1981] and *Jacobs* [1984]; data for Figure 2c are from *Jacobs* [1984] and *Scranton et al.* [1987]; data for Figure 2d are from *Jacobs* [1984] and *Shipboard Scientific Party* [1998]; and data for Figure 2e are from *Chapman and Bailey* [1991] and *Waldron and Probyn* [1991].

the adjacent Caribbean Sea. During lowstands such as that of the last glaciation maximum, exchange was dominated by nutrient-poor surface waters, limiting primary productivity and lessening oxygen demand in the deepwater mass. As sea level rose during the postglacial period, nutrient-rich intermediate waters entered the basin, stimulating primary productivity and increasing deepwater oxygen demand from about ~14.5 ka [*Peterson et al.*, 1991; *Haug et al.*, 1998; *Werne et al.*, 2000; *Lyons et al.*, 2003]. Since then, deepwaters of the Cariaco Basin have been persistently euxinic although subject to small, decadal- to millennial-scale fluctuations in redox potential [*Scranton et al.*, 1987, 2001; *Zhang and Millero*, 1993; *Dean et al.*, 1999; *Piper and Dean*, 2002]. Rates of bulk sediment (80–250 g m^{-2} yr^{-1}) and organic carbon accumulation (10–60 g m^{-2} yr^{-1}) are moderate (Table 2), and the sedimentary organic matter is mostly of marine origin [*Wakeham*, 1990; *Fry et al.*, 1991; *Dean et al.*, 1999; *Werne et al.*, 2000; *Müller-Karger et al.*, 2001; *Lyons et al.*, 2003].

2.1.4. Saanich Inlet

[10] Saanich Inlet is a 45-km^2 fjord at the southeastern end of Vancouver Island, Canada, connected through the

Table 2. Aqueous and Sedimentary Chemical Parameters of Modern Anoxic Marine Environments[a]

	Deepwater $[H_2S]_j$, $\mu mol\ L^{-1}$	Deepwater $[Mo]_{aq}$, $nmol\ L^{-1}$	Deepwater $[Mo]_{aq}$[b]	Bulk Sediment Burial Flux, $g\ m^{-2}\ yr^{-1}$	Organic C Burial Flux, $g\ m^{-2}\ yr^{-1}$	Mo Burial Flux,[b] $mmol\ m^{-2}\ yr^{-1}$	TOC,[c] %	Mo,[c] ppm	$[Mo]_s/TOC$, $\times 10^{-4}$
Black Sea[d]	350	0.2–0.3	0.03–0.05	10–200	1–10	0.02 (0.12)	6.1 (17.3)	45 (190)	4.5 ± 1
Framvaren Fjord[e]	6000–8400	1.3–2.2	0.20–0.30	50–120	12–24	0.20 (0.24)	11.6 (18.6)	84 (265)	9 ± 2
Cariaco Basin[f]	60	6.8–8.4	0.70–0.85	80–250	10–60	0.63 (1.93)	4.4 (6.2)	85 (187)	25 ± 5
Saanich Inlet[g]	25	7.2–9.6	0.80–1.0	420–4800	20–110	0.62 (1.01)	3.2 (5.3)	21 (126)	45 ± 5
Namibian Shelf[h]	~0	10.5[i]	1.0[i]	120–800	10–100	0.16 (0.66)	6.7 (22.3)	33 (142)	6 ± 3

[a]Subscript aq, aqueous; subscript s, sediment.
[b]Aqueous Mo concentrations relative to seawater on a salinity-normalized basis, i.e., $[Mo/Cl]/[Mo/Cl]_{seawater}$.
[c]Average values, with maximum values in parentheses.
[d]*Hirst* [1974], *Shimkus and Trimonis* [1974], *Volkov and Fomina* [1974], *Brumsack* [1989], *Ravizza et al.* [1991], *Karl and Knauer* [1991], *Lyons* [1992], and *Arthur et al.* [1994].
[e]*Skei* [1981, 1983, 1986], *Landing and Westerlund* [1988], *Naes et al.* [1988], *Yao and Millero* [1995], and *Dyrssen et al.* [1996].
[f]*Zhang and Millero* [1993], *Yarincik et al.* [2000], *Piper and Dean* [2002], and *Lyons et al.* [2003].
[g]*François* [1987] and *Shipboard Scientific Party* [1998].
[h]*Brongersma-Sanders et al.* [1980] and *Calvert and Price* [1983].
[i]Assumed equal to unmodified seawater.

shallow Satellite Channel to the deeper Georgia and Haro straits (Figure 1d). It has a maximum depth of 238 m and a sill at 70 m that limits deepwater exchange (Table 1 and Figure 2d) [*François*, 1987]. The low-salinity surface water layer to ~10 m is maintained mainly by runoff from the Cowichan River, which enters Cowichan Bay 6 km northwest of the sill, and the intermediate water layer to ~50 m is maintained by freshets from the Fraser River, which flows into the Georgia Strait 50 km to the northeast (Figure 1d). Compared with discharge from the Cowichan River (5–90 $m^3\ s^{-1}$), that from the Goldstream River at the fjord's head is insignificant (<1 $m^3\ s^{-1}$). As a consequence, the overall circulation pattern is "reverse estuarine," with surface water influx at the mouth rather than the head of the fjord [*François*, 1987]. Because deepwater renewal occurs during most years, much of the deep basin is only seasonally anoxic, and both the depth of the chemocline (~150–238 m) and the redox potential of the deepwater layer ($[H_2S]_{aq}$ 0–25 $\mu mol\ L^{-1}$) vary considerably (Figure 2d) [*Anderson and Devol*, 1973; *Jacobs*, 1984; *François*, 1987; *Shipboard Scientific Party*, 1998; *Russell and Morford*, 2001]. Deepwater anoxia in Saanich Inlet developed through stepwise declines in redox potential at ~12.5 and ~7 ka, resulting in replacement of homogenous C_{org}-poor muds with varved, organic-rich diatomaceous sediments [*Shipboard Scientific Party*, 1998; *Morford et al.*, 2001]. Compared to other modern anoxic marine environments, Saanich Inlet exhibits exceptionally high rates of organic carbon (20–110 g $m^{-2}\ yr^{-1}$) and bulk sediment accumulation (420–4800 g $m^{-2}\ yr^{-1}$; Table 2) [*François*, 1988; *Shipboard Scientific Party*, 1998].

2.1.5. Namibian Shelf

[11] The 30- to 150-km-wide continental shelf of Namibia (southwest Africa) is characterized by strong upwelling and high primary productivity associated with the Benguela Current (Figure 1e). At least six major upwelling cells are located between Cape Frio, Angola in the north (18°30′S) and Cape Town, South Africa, in the south (34°00′S) and are controlled by submarine and coastal topography and their influence on shelf currents [*Chapman and Bailey*, 1991]. Walvis Bay, located along the northwest Namibian coast, is the center of one of the most oxygen-depleted cells, averaging <22 $\mu mol\ O_2\ L^{-1}$ in a coastal strip about 400 km long and 50 km wide (Figures 1e and 2e) [*Price and Calvert*, 1973; *Dingle and Nelson*, 1993]. Depletion of dissolved oxygen is not controlled by topographic barriers to circulation since the shelf lacks a sill; rather, oxygen deficiency is maintained dynamically through a combination of upwelling of suboxic waters from the oxygen minimum zone below the shelf margin and respiratory oxygen demand associated with upwelling-stimulated primary productivity [*Chapman and Shannon*, 1985; *Dingle and Nelson*, 1993]. Upwelling along the Namibian Shelf is a quasi-seasonal phenomenon related to variations in wind stress and generally peaks between November and March [*Chapman and Shannon*, 1985]. Rates of organic carbon (10–100 g $m^{-2}\ yr^{-1}$) and bulk sediment accumulation (120–800 g $m^{-2}\ yr^{-1}$) are moderate to high within Walvis Bay (Table 2), but these values decrease by at least an order

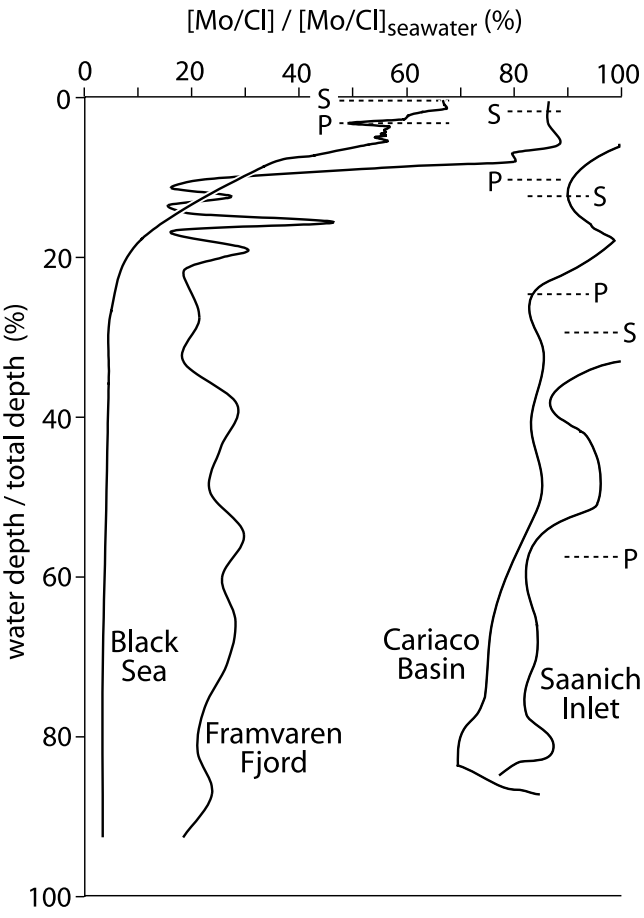

Figure 3. Comparative $[Mo]^*_{aq}$ profiles for modern anoxic silled-basin environments, modified from Figure 2. Aqueous Mo concentrations are given on a seawater-normalized basis to correct for salinity differences among environments; water depth is normalized to total depth for each basin to facilitate comparisons. Basin sill (S) and water column pycnocline (P) depths are shown for each environment.

of magnitude offshore on the upper continental slope [*Veeh et al.*, 1974; *Brongersma-Sanders et al.*, 1980; *Calvert and Price*, 1983].

2.2. Aqueous Chemistry

2.2.1. Redox Profiles

[12] The modern anoxic marine environments examined in this study exhibit depth-dependent variation in redox potential (Figure 2 and Table 2). In the four silled basins, $[O_2]_{aq}$ decreases from surface values that are in approximate equilibrium with the atmosphere to zero at the chemocline. Below the chemocline, $[H_2S]_{aq}$ increases downward from zero to a maximum at the seafloor that varies from ~0–25 μmol L^{-1} for Saanich Inlet to ~6000–8400 μmol L^{-1} for Framvaren Fjord. The rate of increase in $[H_2S]_{aq}$ with depth is nonlinear and generally greatest just below the chemocline, whereas the deeper part of the water column may exhibit nearly uniform H_2S concentrations, as in the Black Sea (Figure 2a). Chemocline depth is shallowest in Framvaren Fjord (18 m) and deepest in the Cariaco Basin (250–375 m; Figures 2b and 2c). However, on a depth-normalized basis (i.e., chemocline depth/total basin depth), the chemocline is shallowest in the Black Sea (0.02–0.06), followed by Framvaren Fjord (0.10–0.11), the Cariaco Basin (0.18–0.26), and Saanich Inlet (0.63–1.0; Figure 3 and Table 1). On the Namibian Shelf, the chemocline only rarely rises above the sediment-water interface, so its "chemocline depth ratio" is effectively 1.0. Chemocline depth ratios provide a measure of the relative degree of deepwater restriction in the study environments. They are also linked to chemocline stability, which decreases for environments with greater relative chemocline depths. Thus the Black Sea and Framvaren Fjord have comparatively stable chemoclines, whereas Saanich Inlet exhibits large fluctuations in chemocline depth on a seasonal timescale (Figure 2d).

2.2.2. Aqueous Mo Profiles

[13] The four anoxic silled basins of the present study exhibit depth-dependent variation in aqueous Mo concentrations, $[Mo]^*_{aq}$ (the asterisk indicates normalization of concentration data to seawater salinity, i.e., $[Mo/Cl]/[Mo/Cl]_{seawater}$ [cf. *Emerson and Huested*, 1991]) (Figure 2). Surface water $[Mo]^*_{aq}$ values range from ~0.7 in the Black Sea (i.e., 70% of the Mo concentration of seawater on a salinity-normalized basis) to ~0.9 in Framvaren Fjord and 1.0 in the Cariaco Basin and Saanich Inlet. In all basins, $[Mo]^*_{aq}$ exhibits a first-order decrease with increasing water depth, although small-scale variation is evident in some basins (e.g., Framvaren Fjord, Figure 2b). The degree of deepwater $[Mo]^*_{aq}$ depletion is greatest in the Black Sea (0.02–0.03) and Framvaren Fjord (0.20–0.30), whereas only moderate decreases are registered by the Cariaco Basin (0.70–0.85) and Saanich Inlet (0.80–1.0, Figure 2 and Table 2). With increasing restriction of the subpycnoclinal water mass, $[Mo]^*_{aq}$ profiles become more nonlinear; most of the reduction in $[Mo]^*_{aq}$ is focused in a narrow vertical range close to the chemocline, and the deeper water column exhibits nearly uniform concentrations (e.g., the Black Sea, Figure 2a). In contrast, in less restricted environments $[Mo]^*_{aq}$ declines more or less continuously with depth throughout the subchemoclinal water mass (e.g., the Cariaco Basin and Saanich Inlet; Figures 2c and 2d). No $[Mo]_{aq}$ data are available for the Namibian Shelf, but it is unlikely that any measurable variation exists in an open marine setting with unrestricted circulation.

[14] Certain features of their aqueous Mo profiles may provide information regarding patterns of deepwater renewal in these silled anoxic basins (see below). In the Black Sea, uniform $[Mo]^*_{aq}$ values below ~500 m suggest no recent, large-scale penetration of Mo-bearing waters from above the chemocline or outside the basin (Figure 2a). In Framvaren Fjord, variation in $[Mo]^*_{aq}$ in discrete layers between 20 and 40 m may be due to relatively recent renewal of the intermediate-depth water mass through hyperpycnal overspills that descended to specific density compensation depths, a process known as "interleaving" (Figure 2b) [*Skei*, 1983, 1986; *Stigebrandt and Molvaer*, 1988; *Dyrssen et al.*, 1996]. In the Cariaco Basin and Saanich Inlet, relatively uniform $[Mo]^*_{aq}$ variation

with depth implies continuous vertical mixing across the chemocline, although local spikes in $[Mo]_{aq}$* values at 200–300 m in the Cariaco Basin and at 90–130 m in Saanich Inlet may be evidence of recent incursions of hyperpycnal water masses into these basins (Figures 2c and 2d). The relationship of variation in aqueous Mo profiles to deepwater renewal events remains tentative owing to insufficient historical data from most of the study environments to document the latter.

2.2.3. Basin Geometry and Deepwater Restriction

[15] Variation in redox and aqueous Mo profiles among modern anoxic marine systems can be related directly to basin geometry and its influence on deepwater restriction. Basin-margin sills, which control the influx of oxygenated, non-Mo-depleted waters, range in depth from 2–2.5 m in Framvaren Fjord to 146 m in the Cariaco Basin (Figure 2). However, absolute sill depth is less important than the ratio of sill depth to total basin depth, because the "sill depth ratio" is dimensionally related to aspects of basin geometry that control the overall rate of deepwater renewal, e.g., the cross-sectional area of the sill and the total volume of the basin (Table 1). The smallest sill depth ratios are encountered in the Black Sea and Framvaren Fjord (0.01–0.02), followed by the Cariaco Basin (0.10) and Saanich Inlet (0.29, Figure 3); the Namibian Shelf, lacking a sill, has a nominal sill depth ratio of 1.0. For the anoxic marine environments considered here, sill depth ratio correlates positively with deepwater $[Mo]_{aq}$* and negatively with deepwater renewal time, τ_{dw} (Tables 1–2), demonstrating a relationship between basin geometry and aqueous chemical and physical properties. The relationship to deepwater renewal time is particularly significant as it represents a direct measure of the degree of restriction of the subchemoclinal water mass.

2.2.4. Deepwater Ages

[16] All silled marine basins are subject to deepwater renewal events that introduce variable quantities of dissolved oxygen into the oxygen-deficient and commonly sulfidic subchemoclinal water mass. If deep waters are depleted in aqueous trace metal species such as MoO_4^{2-}, then these will be resupplied during such events as well. Processes that effectuate deepwater renewal include hyperpycnal overspills at marginal sills, water column overturn (e.g., via surface cooling), turbulent vertical mixing (e.g., via storms), and density flows generated around basin margins as a function of slope instability, seismicity, or human activity [e.g., *Gade and Edwards*, 1980; *Molvaer*, 1980; *Magyar et al.*, 1993]. Such processes have been documented or inferred to operate in all of the silled marine basins of the present study, although their relative importance varies among environments as a function of basin configuration and hydrographic and tectonic factors [e.g., *Anderson and Devol*, 1973; *Skei*, 1983; *Östlund and Dyrssen*, 1986; *Stigebrandt and Molvaer*, 1988; *Friedrich and Stanev*, 1989; *Holmen and Rooth*, 1990; *Lyons*, 1991; *Millero*, 1996; *Scranton et al.*, 2001; *Popescu et al.*, 2004]. The influence of these processes on deepwater chemistry depends on the scale and frequency of renewal events relative to the volume of the subchemoclinal water mass: for large basins such as the Black Sea, the effects are attenuated by basin size. Historical data can track the influence of even relatively minor renewal events on deepwater chemistry [e.g., *Matthäus*, 1995], but owing to time-averaging processes in the sediment only relatively large events are likely to leave a recognizable imprint in the stratigraphic record.

[17] The scale of deepwater renewal in a given environment is reflected in its "age" or renewal time, τ_{dw} (the term "residence time" is more appropriately reserved for aqueous chemical species). Several types of age tracers are available: (1) radioisotopes such as ^{14}C and ^{3}H (tritium) that are mixed downward from the atmosphere-water interface and that decay at a known rate and (2) isotopic tracers that diffuse into the water column from the sediment (e.g., ^{3}He, ^{226}Ra), producing vertical concentration gradients from which age models can be generated. Existing age-tracer data are sparse for some of the study environments, and where multiple techniques have been employed, the results are not always in agreement. For the Black Sea, radiocarbon analysis yields τ_{dw} estimates of 1000–1500 years and ~2000 years for intermediate and deep waters, respectively, although shorter τ_{dw} values have been calculated from ^{3}He and ^{226}Ra profiles (~500–1000 years) and hydrographic modeling (387 years) [*Östlund*, 1974; *Östlund and Dyrssen*, 1986; *Top et al.*, 1990; *Murray et al.*, 1991; *Falkner et al.*, 1991; *Dyrssen et al.*, 1996; *Dyrssen*, 1999]. The vertical age structure of the Black Sea water column is thought to reflect penetration of saline Mediterranean inflows to intermediate water depths [*Murray et al.*, 1991]; the process responsible for transfer of limited quantities of ^{3}H below 1700 m [*Top and Clarke*, 1983] is uncertain. The τ_{dw} of Framvaren Fjord deepwaters was estimated at ~1600 years by ^{14}C analysis [*Dyrssen et al.*, 1996; *Dyrssen*, 1999], but other age tracers have generally yielded younger estimates. Both intermediate (20–100 m) and deep waters (>100 m) in Framvaren contain measurable levels of tritium (4–10 and 0.1–0.8 tritium units, respectively, versus 1989–1992 surface water reference values of 10.8–12.8 tritium units), implying renewal times on the order of <15 years and ~50–100 years, respectively [*Dyrssen et al.*, 1996]. A similar estimate of τ_{dw} (123 ± 9 years) for Framvaren was obtained from modeling of an aqueous silica concentration profile [*Yao and Millero*, 1995]. Cariaco Basin deep waters have been dated by ^{14}C analysis at ~100 years [*Deuser*, 1973]. No age tracer studies have been carried out in Saanich Inlet or on the Namibian Shelf.

[18] Another approach to estimation of deepwater renewal times is based on trace metal flux calculations [cf. *Colodner et al.*, 1995]:

$$\tau_{dw} = \left[\left(1 - [Mo]^*_{aq}\right) \times [Mo]_{sw} \times S_{dw}/S_{sw} \times V \times \rho_{dw}\right] / (f(Mo) \times A), \quad (1)$$

where $[Mo]^*_{aq}$ is the seawater-normalized deepwater Mo concentration (dimensionless), $[Mo]_{sw}$ is seawater Mo concentration (in mmol kg^{-1}), S_{dw} and S_{sw} are the salinities of deepwater and seawater, respectively, ρ_{dw} is deepwater

density (in kg m^{-3}), f(Mo) is Mo burial flux (in mmol m^{-2} yr^{-1}), and A and V are basin area and volume (in m^2 and m^3, respectively; see Tables 1 and 2 for environment-specific data). Equation (1) effectively represents the ratio of the mass of Mo extracted from a given deepwater mass to the rate at which it is extracted. Most of the input variables are well constrained for the study environments, although some degree of uncertainty is associated with Mo burial fluxes, which depend on sediment depth-time models that are only approximately known for some environments.

[19] Estimates of τ_{dw} based on trace metal fluxes are useful in providing an independent check on the results of other techniques and a first approximation when other age tracers are unavailable. Using equation (1), we calculated values of τ_{dw} for the Black Sea, Framvaren Fjord, and the Cariaco Basin that, allowing for a twofold uncertainty in Mo burial fluxes, are in agreement with estimates based on tracer studies. Our τ_{dw} value for the Black Sea (3950 years) supports published ^{14}C deepwater ages of ~2000 years [*Östlund and Dyrssen*, 1986] and suggests that younger ages based on ^{3}He and ^{226}Ra profiles may be problematic [cf. *Anderson and Fleisher*, 1991; *Colodner et al.*, 1995], although it is possible that the ^{14}C ages are skewed by excess "dead" dissolved inorganic carbon [*Murray et al.*, 1991]. Our τ_{dw} value for Framvaren Fjord (50 years) is close to estimates based on tritium concentrations (50–100 years) and Si profile modeling (123 ± 9 years), suggesting that much older published ^{14}C ages (~1600 years) are anomalous [*Dyrssen et al.*, 1996; *Dyrssen*, 1999]. The shorter age estimates are consistent with historical records of hydrographic events in Framvaren Fjord (i.e., the 1853 sill dredging and 1902 sill deepening) that are thought to have resulted in near-total renewal of Framvaren deep waters [*Skei*, 1988; *Anderson et al.*, 1988]. Our τ_{dw} value for the Cariaco Basin (52 years) is close to a published ^{14}C age of ~100 years [*Deuser*, 1973], which is consistent with a major deepwater renewal event around 1915–1920 inferred on the basis of secular increases in H_2S and NH_4^+ concentrations [*Millero*, 1996]. Other evidence in support of relatively recent deepwater exchange in the Cariaco Basin includes the presence of sulfite and thiosulfate (products of partial oxidation of H_2S) and tritium ($\lambda_{1/2}$ = 12.3 years) in the subchemoclinal water mass [*Holmen and Rooth*, 1990; *Zhang and Millero*, 1993; *Millero*, 1996].

[20] We also used trace metal flux data to calculate τ_{dw} values of 1.5 years for Saanich Inlet and 0 years for the Namibian Shelf, which are consistent with the relatively open character of these environments and their known deepwater renewal patterns. In Saanich Inlet, deepwater renewal takes place when the density of the subpycnoclinal water mass is exceeded by that of surface waters in nearby Haro Strait [*Anderson and Devol*, 1973; *François*, 1987; *Shipboard Scientific Party*, 1998; *Russell and Morford*, 2001]. Such renewal events occur mainly during the late summer and autumn when freshwater runoff is at a minimum, with individual events controlled by fortnightly tidal mixing and lasting 8 to 10 days. Renewal of Saanich deep waters to a depth of 100 m occurs annually, but renewal events reaching 200 m occur more irregularly and in only about one year out of two. A consequence of these renewal patterns is that both the depth of the chemocline (~150–238 m) and the redox potential of the deepwater layer ($[H_2S]_{aq}$ 0–25 μmol L^{-1}) exhibit considerable interannual variability (Figure 2d) [*Jacobs*, 1984; *François*, 1987; *Shipboard Scientific Party*, 1998]. On the other hand, upwelling onto the Namibian Shelf is a more or less continuous phenomenon. Because upwelling waters have been out of contact with the atmosphere for an extended interval, they are suboxic and yield ^{14}C ages on the order of hundreds of years [*Millero*, 1996]. Despite such "aging," the dissolved Mo concentrations of these waters are unlikely to be depleted relative to normal seawater concentrations, an inference consistent with trace metal–based age estimates that are effectively zero.

2.3. Sediment Geochemistry

2.3.1. Data Sources and Reporting Conventions

[21] Sedimentary Mo and TOC data for the modern anoxic marine environments examined in this study were compiled from published sources except for the Black Sea data set shown in Figure 4. We report $[Mo]_s$ as raw values rather than on an Al-normalized basis, as in many studies. Although Al normalization yields an "enrichment factor" that is useful in facilitating comparisons between facies, particularly when dilution by biogenic components is severe [e.g., *Brumsack*, 1989; *Piper*, 1994; *Dean et al.*, 1997, 1999], it serves no purpose when examining intraformational variation of a trace element relative to TOC. Both are subject to dilution by mineral phases, and use of Al-normalized concentrations for trace elements and raw concentrations for TOC can lead to introduction of unwanted variance in trace element–TOC relationships (note that interested readers are encouraged to correspond with the authors on this topic). Although geochemical studies commonly present sediment core data in the form of chemostratigraphic diagrams (e.g., Figure 4), we have found crossplots to be especially useful in visualizing Mo-TOC relationships (e.g., Figure 5). These plots allow comparison of surface sample and sediment core data in a common format, in which stratigraphic information from core samples can be represented as "covariation paths" (e.g., Figures 5b and 5c). As shown below, such crossplots can be highly effective at revealing patterns of Mo-TOC covariation that have potential environmental significance. A concern in analyzing core data from geologically young sediments is that stratigraphic trends in organic carbon concentration may be influenced by ongoing diagenetic processes, e.g., bacterially mediated redox reactions, resulting in a progressive loss of organic carbon downward from the sediment-water interface. However, for reasons discussed below, we do not think that such processes have resulted in a diagenetic overprint that obscures a primary environmental signal in the study units.

2.3.2. Black Sea

[22] The Black Sea has been the focus of a number of oceanographic expeditions, e.g., the 1969 *Atlantis II*

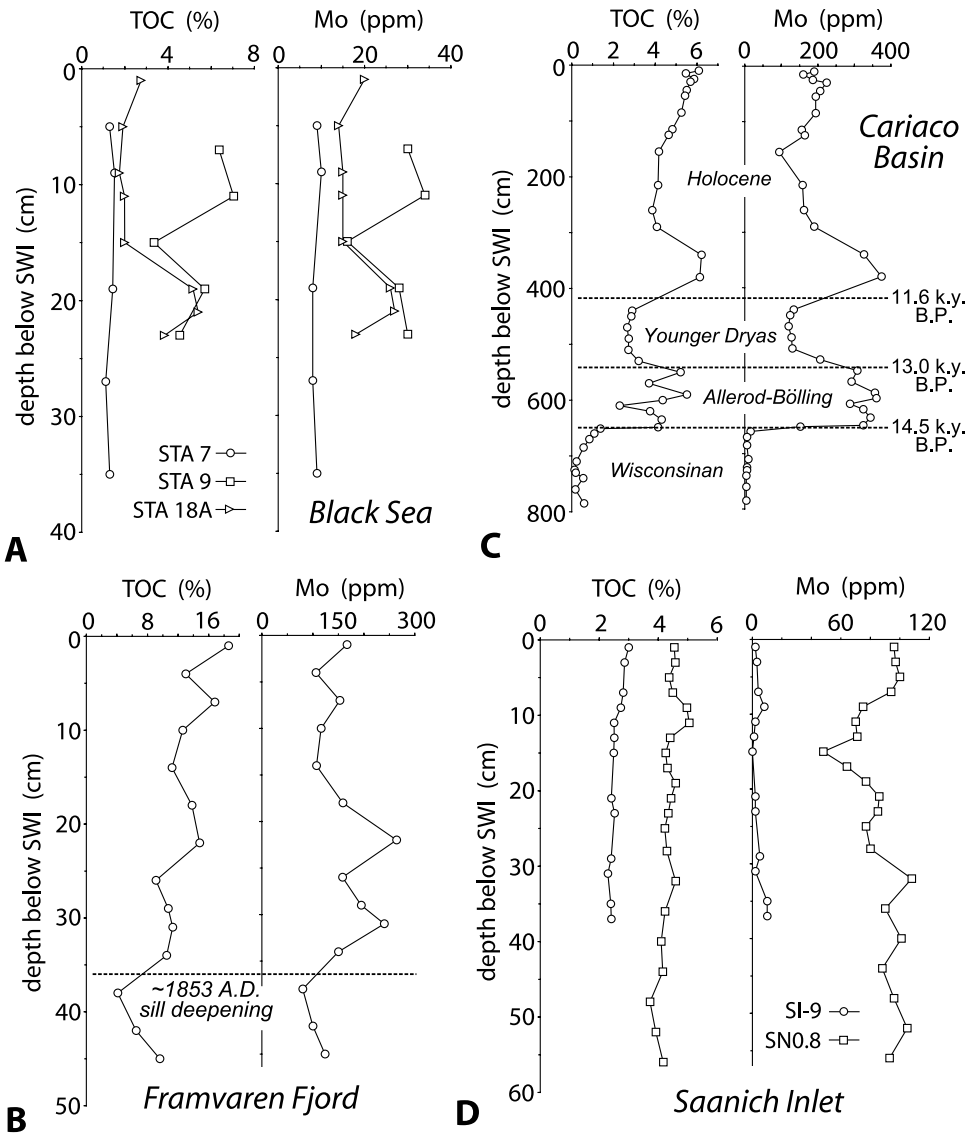

Figure 4. Sediment [Mo] and total organic carbon (TOC) versus depth below the sediment-water interface for modern anoxic silled-basin environments: (a) Black Sea, (b) Framvaren Fjord, (c) Cariaco Basin, and (d) Saanich Inlet. Stratigraphic position and ages of major hydrographic events are shown in Figures 4b and 4c. Data source for Figure 4a is T. W. Lyons (unpublished data, 2005); data sources for Figure 4b is *Skei* [1981] and *Skei et al.* [1988]; data source for Figure 4c is *Lyons et al.* [2003]; and data source for Figure 4d is *François* [1987]. For the Black Sea samples, TOC and Mo concentrations were analyzed by coulometry and inductively coupled plasma-emission spectroscopy, respectively; see *Lyons et al.* [2003] for methodological details.

[*Degens and Ross*, 1974] and 1988 R/V *Knorr* cruises [*Murray*, 1991b], resulting in collection of shallow gravity and box cores from many sites across the basin [e.g., *Hirst*, 1974; *Volkov and Fomina*, 1974; *Brumsack*, 1989; *Ravizza et al.*, 1991; *Lyons*, 1991]. These cores have revealed a sequence of three major sedimentary units (from the surface downward): (1) unit 1, a 30- to 50-cm-thick, laminated, white-brown organic coccolith ooze younger than ~1320 years B.P.; (2) unit 2, a ~50-cm-thick, laminated, olive-black marine sapropel; and (3) unit 3, a lacustrine mudstone deposited prior to the Holocene marine incursion at ~7540 years B.P. [*Arthur et al.*, 1994; *Jones and Gagnon*, 1994]. Intercalated within units 1 and 2 are homogeneous, greenish-gray mud layers up to 20 cm thick that have been termed "turbidites," although the lack of basal erosion draws into question the exact mode of emplacement [*Lyons*, 1991; *Arthur et al.*, 1994].

[23] Compilation of published $[Mo]_s$-TOC data regardless of sample location or age yields a diffuse distribution with moderate clustering in the low-TOC range and an average $[Mo]_s$/TOC ratio of ~8 ± 4, although the low-TOC samples appear to yield a somewhat higher ratio and the high-TOC

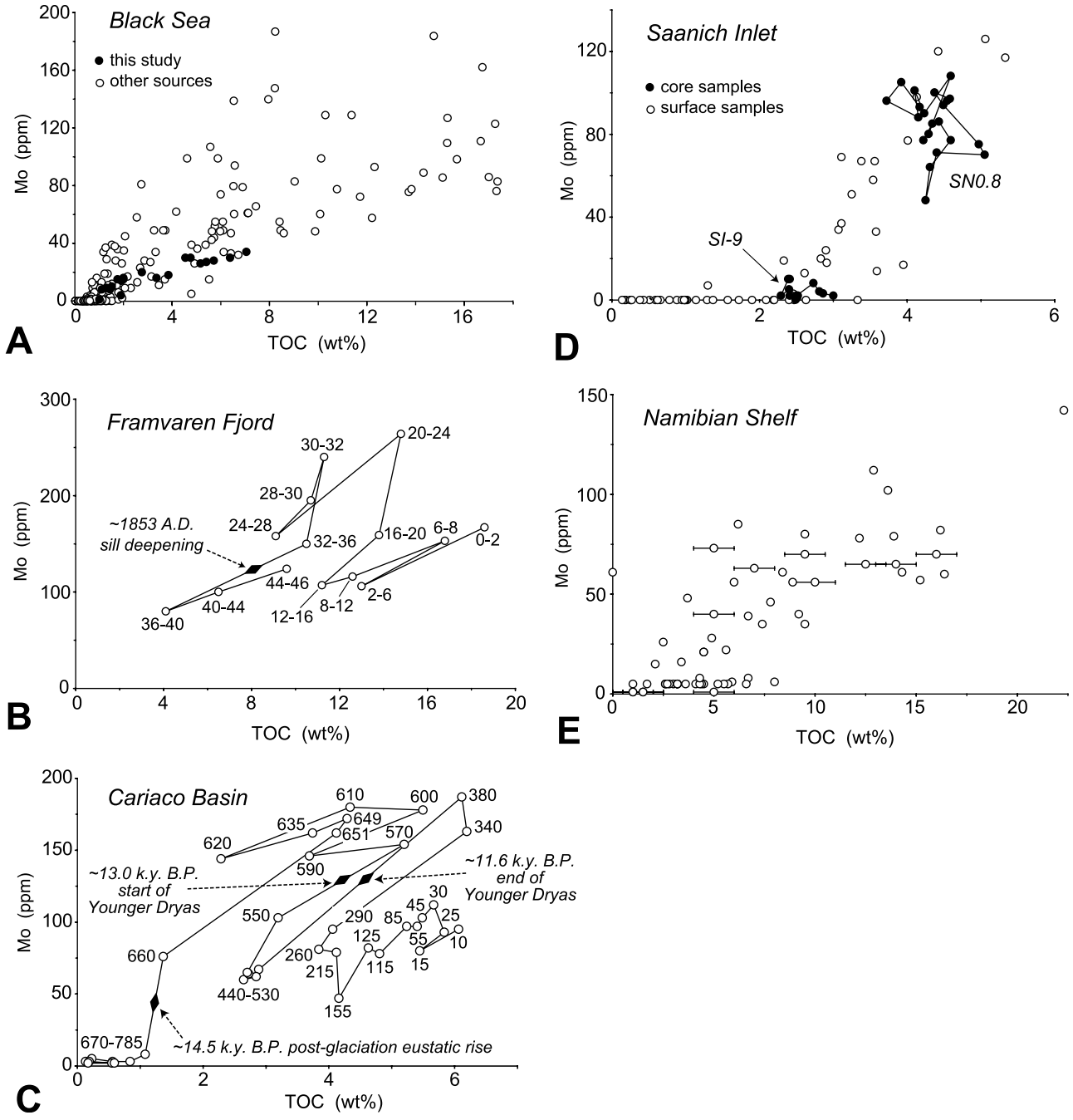

Figure 5. Sediment [Mo] versus TOC for modern anoxic marine environments: (a) Black Sea, (b) Framvaren Fjord, (c) Cariaco Basin, (d) Saanich Inlet, and (e) Namibian Shelf. In Figures 5b and 5c, numbers indicate sample depth in centimeters below the sediment-water interface, and the stratigraphic position and ages of major hydrographic events are shown. Additional data not referenced in Figure 4 are from *Hirst* [1974], *Volkov and Fomina* [1974], *Brumsack* [1989], and *Ravizza et al.* [1991] for Figure 5a; from *François* [1987] for Figure 5d; and from *Brongersma-Sanders et al.* [1980] and *Calvert and Price* [1983] for Figure 5e (note that Brongersma-Sanders et al. samples have error bars reflecting uncertainty of TOC estimates).

samples a somewhat lower ratio (Figure 5a). Analysis of the sediment data by water depth revealed a slight yet statistically significant decrease in $[Mo]_s$/TOC ratios from $\sim 12 \pm 6$ at 500 m to $\sim 8 \pm 4$ below 2000 m (not shown), whereas analysis by sample depth below the sediment-water interface yielded no trend within units 1 and 2. Although these existing data are probably all analytically valid, they represent many different locales and offer low stratigraphic

resolution at best, factors that may obscure fundamental Mo-TOC relationships. To test whether more coherent patterns might be apparent in high-resolution, single-site chemostratigraphic data sets, we generated Mo-TOC data at 2-cm intervals from box cores taken at stations 7, 9, and 18A (Figure 4a) (see Figure 1a and *Lyons* [1991] for station locations and descriptions). The core from station 7, at a depth of 1950 m in a toe-of-slope setting northeast of the Bosporus, consists of 36 cm of "turbidites" with limited calcareous ooze. The core from station 9, at 2095 m on the central abyssal plain, consists of 24 cm of unit 1 coccolithic ooze, while that from station 18A, at 2150 m on the central abyssal plain, yielded 8 cm of the coccolithic ooze overlain by a 16-cm-thick "turbidite" (see *Lyons* [1991, 1997] and *Lyons and Berner* [1992] for further lithologic details). On a Mo-TOC crossplot, this sample set yields a tight linear array with a slope of ~4.5 ± 1 (Figure 5a).

2.3.3. Framvaren Fjord

[24] The Norwegian Institute for Water Research (NIVA) has collected and analyzed several gravity cores from Framvaren Fjord [*Skei*, 1981, 1986; *Skei et al.*, 1988], although the number is insufficient for an assessment of spatial variation in sediment geochemistry. The $[Mo]_s$-TOC data reproduced here were generated at 2- to 4-cm intervals in the 46-cm-long core F1, located in the deepest part of the fjord (Figure 1b); this interval is estimated to represent the last ~250 years, although part of the surface "fluff" layer at the sediment-water interface may not have been recovered. A sharp contact at ~36 cm below the sediment-water interface separates laminated black muds from underlying green muds (Figure 4b). This contact represents the sedimentary record of sill excavation in ~1853 A.D. [*Skei*, 1983, 1986].

[25] The black muds, which are markedly enriched in both Mo and TOC relative to the older green muds, exhibit a distinctive pattern of Mo-TOC covariation (Figure 4b). An initial increase in $[Mo]_s$ at 30–36 cm is accompanied by only a limited increase in TOC, followed by increases in both $[Mo]_s$ and TOC (20–30 cm) and then by irregular fluctuations with a general trend toward lower $[Mo]_s$ and higher TOC values (0–20 cm; Figure 5b). Despite the serpentine character of the "covariation path" shown in Figure 5b, most of the sample-to-sample changes in $[Mo]_s$ and TOC concentrations are marked by positive covariation. Owing to the concurrent upsection decrease in $[Mo]_s$ and increase in TOC noted above, the slope of the $[Mo]_s$-TOC relationship changes from ~20 at 20–30 cm to ~9 at 0–16 cm (Figure 5b).

2.3.4. Cariaco Basin

[26] The Cariaco Basin section, first studied in piston cores during the 1950s and in detail during subsequent cruises [e.g., *Peterson et al.*, 1991], was recovered in a long drill core from Site 1002 of the Ocean Drilling Program Leg 165 in 1996 (Figure 1c) [*Shipboard Scientific Party*, 1997]. The upper part of this core represents late Pleistocene and Holocene sedimentation, as constrained by a radiocarbon date of ~14.5 ka at 650 cm, just above the glacial/interglacial transition, and dates of ~13.0 ka at 560 cm and ~11.6 ka at 420 cm, bracketing the Younger Dryas interval (Figure 4c, all ages in calendar years [*Hughen et al.*, 1998]). Sediment character changed abruptly at the time of the glacial/interglacial transition, with bioturbated C_{org}-poor clays below ~660 cm yielding to laminated dark-olive-gray C_{org}-rich muds above this level [*Lyons et al.*, 2003]. This transition records a shift from oxic-suboxic to anoxic/euxinic conditions on the seafloor caused by an influx of nutrient-rich intermediate-depth Caribbean Sea waters as sea level rose in the postglacial period [*Haug et al.*, 1998; *Dean et al.*, 1999; *Piper and Dean*, 2002].

[27] A chemostratigraphic plot reveals concurrent changes in $[Mo]_s$ and TOC, with higher values associated with the Allerod-Bölling and early Holocene and lower values with the Wisconsinan and Younger Dryas intervals (Figure 4c). Primary productivity was high during the Younger Dryas, stimulated by the introduction of nutrient-rich intermediate waters associated with rising sea levels or increased upwelling intensity [*Peterson et al.*, 1991; *Dean et al.*, 1999]. During this interval, the burial fluxes of organic matter and biogenic carbonate and opal all increased; lower TOC values are a consequence of the relatively larger increases in biogenic mineral fluxes [*Werne et al.*, 2000; *Lyons et al.*, 2003]. One pattern not readily observed in a chemostratigraphic plot (Figure 4c) but manifested clearly in a $[Mo]_s$-TOC crossplot (Figure 5c) is the long-term trend toward lower $[Mo]_s$ and higher TOC values (0–610 cm) that followed the initial increase in both variables associated with the immediate postglacial sea level rise and the transition from oxic to anoxic facies (610–670 cm). The serpentine trend of this "covariation path" (Figure 5c) is similar to that seen in Framvaren Fjord (Figure 5b). As at Framvaren, sample-to-sample changes in $[Mo]_s$ and TOC concentrations are dominantly characterized by positive covariation (e.g., at 380–570, 260–340, and 30–155 cm), even though the long-term trend toward lower $[Mo]_s$ and higher TOC values represents a negative relationship. Owing to this trend, the slope of the $[Mo]_s$-TOC relationship changes from ~40 at 660–590 cm to ~25 at 155–10 cm (Figure 5c).

2.3.5. Saanich Inlet

[28] Sediment geochemical data for Saanich Inlet are from surface grab samples and short gravity cores analyzed by *François* [1987]. The surface samples were collected from 55 sites distributed throughout the Inlet, whereas the two gravity cores were located in the more restricted inner fjord to the south (SN0.8) and the less restricted outer fjord, proximal to Satellite Channel, in the north (SI-9, Figure 1d). The cores were sampled and analyzed at 2- to 4-cm intervals from the surface to depths of 38 cm (SI-9) and 58 cm (SN0.8, Figure 4d). Given Recent sedimentation rates in Saanich Inlet of ~2–5 mm yr^{-1} [*Shipboard Scientific Party*, 1998], the recovered core intervals may represent only a few hundred years of sediment accumulation.

[29] The surface grab samples reveal significant positive covariation between $[Mo]_s$ and TOC (Figure 5d). Below ~2.5% TOC, $[Mo]_s$ values are uniformly low (<5 ppm), but above this TOC threshold strong Mo enrichment (to 120 ppm) is observed. The latter samples exhibit a $[Mo]_s$/TOC slope of ~45 ± 5 and an x intercept of ~2.5% TOC. Samples from the two gravity cores fall along the $[Mo]_s$-

TOC trend defined by the surface grab samples (Figure 5d). The southern core (SN0.8) yields higher $[Mo]_s$ and TOC values than the northern core (SI-9), but neither core exhibits much stratigraphic variation in sediment geochemistry (Figure 4d). The substantial intersite differences reflect the greater proximity of the northern core to the mouth of the fjord and thus to clastic sources (mainly turbid plumes generated by the Fraser River). These relationships imply a strong geographic gradient in environmental conditions, which has remained nearly constant during the last few hundred years.

2.3.6. Namibian Shelf

[30] Although Namibian Shelf sediments have been collected on a number of expeditions sponsored by American, Dutch, South African, and Russian institutions, publication of integrated geochemical data sets has been rare. The $[Mo]_s$-TOC data reproduced here are from *Brongersma-Sanders et al.* [1980] and *Calvert and Price* [1983]. The Brongersma-Sanders et al. study was based on 13 gravity cores taken on the continental shelf between Henties Bay in the north and Walvis Bay in the south, spanning a distance of ~100 km, and the Calvert and Price study utilized the surface samples from 52 gravity cores between Dune Point in the north and Sylvia Hill in the south, encompassing ~600 km of continental shelf centered on Walvis Bay (Figure 1e). Because the Brongersma-Sanders et al. data set includes only trace element data, TOC values were estimated for the surface samples from the TOC isopach maps of *Calvert and Price* [1983]. We have not used the subsurface sample data of *Brongersma-Sanders et al.* [1980], for which TOC values are unavailable and cannot be estimated.

[31] Namibian Shelf sediments exhibit a positive although somewhat diffuse relationship between $[Mo]_s$ and TOC (Figure 5e). Mo enrichment above background levels (~3–5 ppm) is limited to samples with higher TOC values: Below 2% TOC no increase is evident, between 2 and 8% TOC about half of the samples show Mo enrichment, and above 8% TOC all samples yield elevated Mo values. It is unclear whether a specific TOC threshold for Mo enrichment exists for the Namibian Shelf, as it does for Saanich Inlet (Figure 5d). The wide geographic distribution of the available sample set may introduce too many diverse influences on $[Mo]_s$ and TOC accumulation to recognize such a threshold, and the lack of a chemostratigraphic data set for the Namibian Shelf precludes evaluation of single-site $[Mo]_s$-TOC relationships. It is also possible that an upwelling zone system characterized by weakly or non-sulfidic bottom waters is unlikely to develop the type of well-defined $[Mo]_s$-TOC relationships observed in other anoxic marine environments of the present study, but further data will be needed to evaluate this issue. The average $[Mo]_s$/TOC ratio for Namibian Shelf sediments is $\sim 6 \pm 3$ (Figure 5e), although, as for the Black Sea (Figure 5a), it is somewhat higher for low-TOC samples and lower for high-TOC samples.

2.3.7. Sampling Protocols and Data Set Parsing

[32] Differences in sample collection protocols among the source studies cited above require comment. A fundamental distinction is whether geochemical data were generated from surface samples or sediment cores: both data types are available for some depositional systems (e.g., Black Sea, Saanich Inlet), whereas only surface sample (e.g., Namibian Shelf) or sediment core data (e.g., Framvaren Fjord, Cariaco Basin) are available for others. This distinction is important because surface samples provide information about spatial (geographic) variation in present-day environmental conditions, whereas core samples provide information about temporal (stratigraphic) variation. In general, variance in sediment geochemistry tends to be minimized for sample sets collected over smaller geographic areas and shorter stratigraphic intervals. These patterns are manifested in the lesser variance of (1) $[Mo]_s$-TOC data for Saanich Inlet (45 km^2) versus the Black Sea (423,000 km^2) (Figures 5a and 5d); (2) site-specific data versus data from all sites in Saanich Inlet or the Black Sea (Figures 5a and 5d); and (3) shorter versus longer stratigraphic intervals of the Framvaren Fjord and Cariaco Basin cores (Figures 5b and 5c). In essence, samples collected over larger spatial and temporal ranges exhibit greater variance because of the potential for influence by a large number of quasi-independent environmental variables, e.g., detrital siliciclastic input, sedimentation rates, and organic matter provenance, among others. In contrast, samples representing a limited stratigraphic interval at a single site are more likely to reflect the effects of a single, dominant environmental parameter (or a few strongly covariant parameters). The geographic and stratigraphic ranges of sampling appear to have a larger influence on $[Mo]_s$-TOC relationships than small-scale variations in lithology, as between unit 1 oozes and turbidites in Black Sea sediment cores (Figure 5a). For these reasons, analysis of relationships between sediment geochemistry and environmental factors is facilitated by restricting the spatial and temporal ranges of the sample sets under investigation. Because environmental (i.e., aqueous chemical) data for the depositional systems under investigation is entirely historical, investigation of the influence of environmental factors on sediment geochemistry is best conducted by limiting data sets to geologically recent samples, i.e., those most likely to have been deposited under environmental conditions similar to the ambient regime.

[33] In view of the considerations above, the $[Mo]_s$-TOC data set for each modern anoxic marine environment of this study was "parsed" to yield a subset representing geologically young samples from a geographically limited area (i.e., one or a few collection sites). The Black Sea data set is especially varied, containing $[Mo]_s$-TOC data from many locales in geographically diverse settings (shelf, slope, basin) [e.g., *Hirst*, 1974; *Volkov and Fomina*, 1974]. The single cores offering the largest number of samples and highest chemostratigraphic resolution are from stations 7, 9, and 18A on the central abyssal plain (Figures 1a, 4a, and 5a) [*Lyons*, 1991]. These exhibit a well-defined relationship between Mo and TOC concentrations, representing a substantial reduction in variance relative to the full, highly heterogeneous geochemical data set for the Black Sea (Figure 5a). $[Mo]_s$-TOC data for Framvaren Fjord and the Cariaco Basin come from single cores (Figures 1b and 1c),

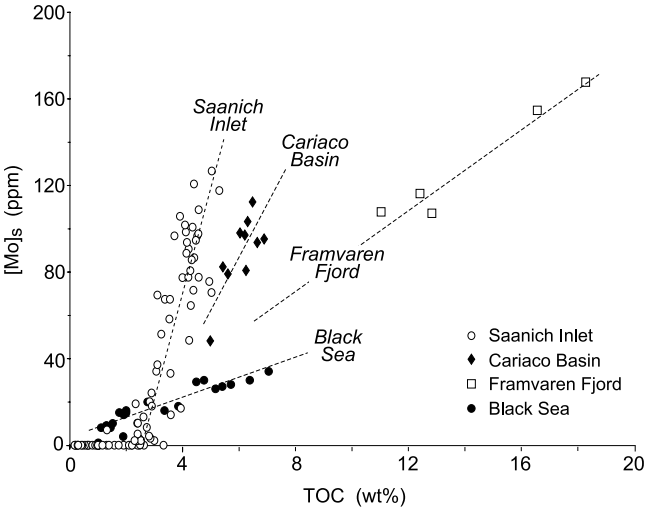

Figure 6. Parsed $[Mo]_s$-TOC data for modern anoxic silled-basin environments. Regression of the data sets (dashed lines) yields the following slopes (m, in units of 10^{-4}): 45 ± 5, Saanich Inlet; 25 ± 5, Cariaco Basin; 9 ± 2, Framvaren Fjord; and 4.5 ± 1 Black Sea. Data are from sources given in Figure 4.

so the parsing procedure simply involved limiting the data sets to the youngest sediment samples, i.e., the 0–16 cm interval of the F1 core (Figures 4b and 5b) and the 0–155 cm interval of the Ocean Drilling Program Site 1002 drill core (Figures 4c and 5c). The Saanich Inlet data set was not parsed owing to the limited spatial and temporal range of the full sample set (Figures 4d and 5d). Finally, the Namibian Shelf data set was not parsed because, being a fully open marine environment, it will not figure into the following discussion of $[Mo]_s$/TOC ratios as a proxy for hydrographic restriction in silled basinal environments. The $[Mo]_s$/TOC ratios of the parsed data sets are 4.5 ± 1 for the Black Sea, 9 ± 2 for Framvaren Fjord, 25 ± 5 for the Cariaco Basin, and 45 ± 5 for Saanich Inlet (Figure 6 and Table 2). Relative to the original data sets, the parsed data sets exhibit marked reductions in variance, suggesting that the latter provide a more coherent representation of $[Mo]_s$-TOC relationships that can be related to ambient environmental conditions.

2.4. Mo and Organic Carbon Burial Fluxes

[34] Mo and TOC burial fluxes and Mo/TOC flux ratios were calculated for the five anoxic marine environments of the present study in order to assess the relationship of sedimentary Mo accumulation to ambient redox conditions and to constrain mechanisms of Mo transfer to the sediment. Mo burial fluxes were calculated as

$$f(\mathrm{Mo}) = [\mathrm{Mo}]_{\mathrm{hydr}} \times \rho_{\mathrm{db}} \times \upsilon \times \psi^{-1} \times \kappa, \qquad (2)$$

where f(Mo) is Mo burial flux in mmol m^{-2} yr^{-1}, $[Mo]_{hydr}$ is the concentration of hydrogenous (i.e., nondetrital) sedimentary Mo (in ppm), ρ_{db} is sediment dry bulk density (in kg m^{-3}), υ is sedimentation rate (in mm yr^{-1}), ψ is the molecular weight of Mo (95.94 g mol^{-1}), and κ is a unit conversion factor equal to 10^{-3}. The hydrogenous Mo concentration, $[Mo]_{hydr}$, was calculated as $[Mo]_s - [Mo]_{detr}/[Al]_{detr} \times [Al]_s$, and detrital Mo and Al concentrations for

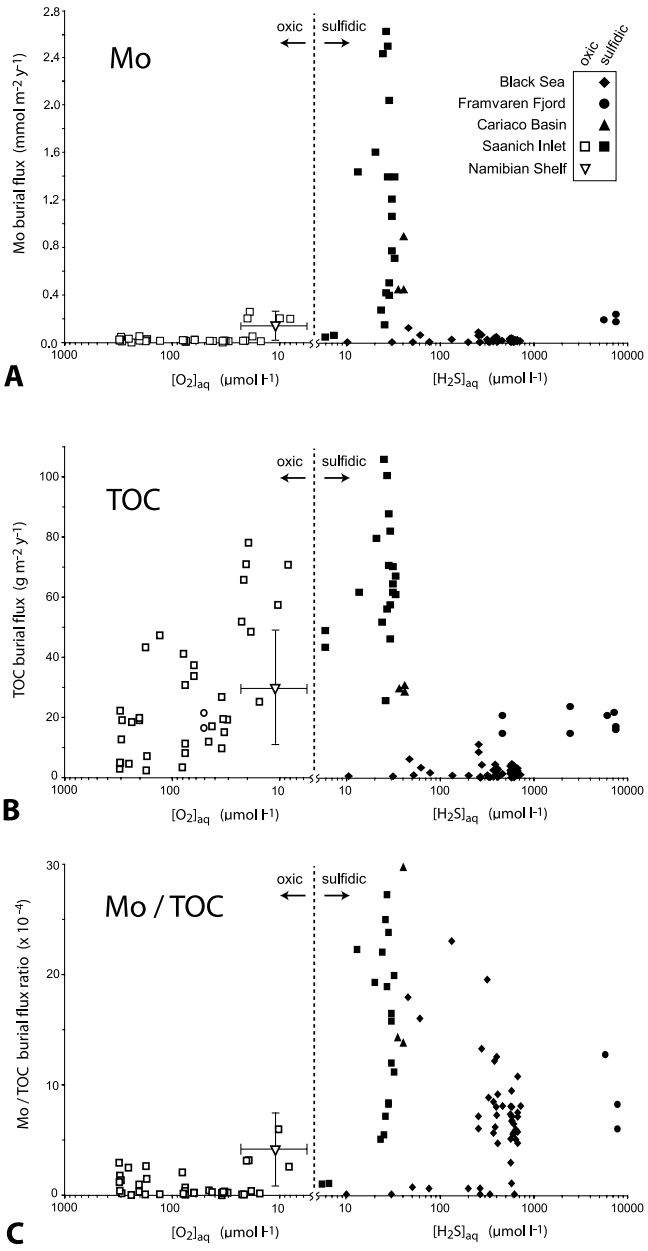

Figure 7. (a) Sedimentary Mo and (b) TOC burial fluxes and (c) Mo/TOC flux ratios versus benthic redox potential for modern anoxic marine environments. Redox potential is represented by logarithmic $[O_2]_{aq}$ and $[H_2S]_{aq}$ scales with more oxic conditions to the left and more sulfidic conditions to the right. Sediment geochemical data are from sources given in Figures 4 and 5, and $[O_2]_{aq}$-$[H_2S]_{aq}$ estimates are based on sample site water depths from these sources and aqueous chemical data from sources given in Figure 2. Data for the Namibian Shelf are plotted as a mean with a standard deviation cross because no site-specific benthic redox data were available. See text for flux calculations.

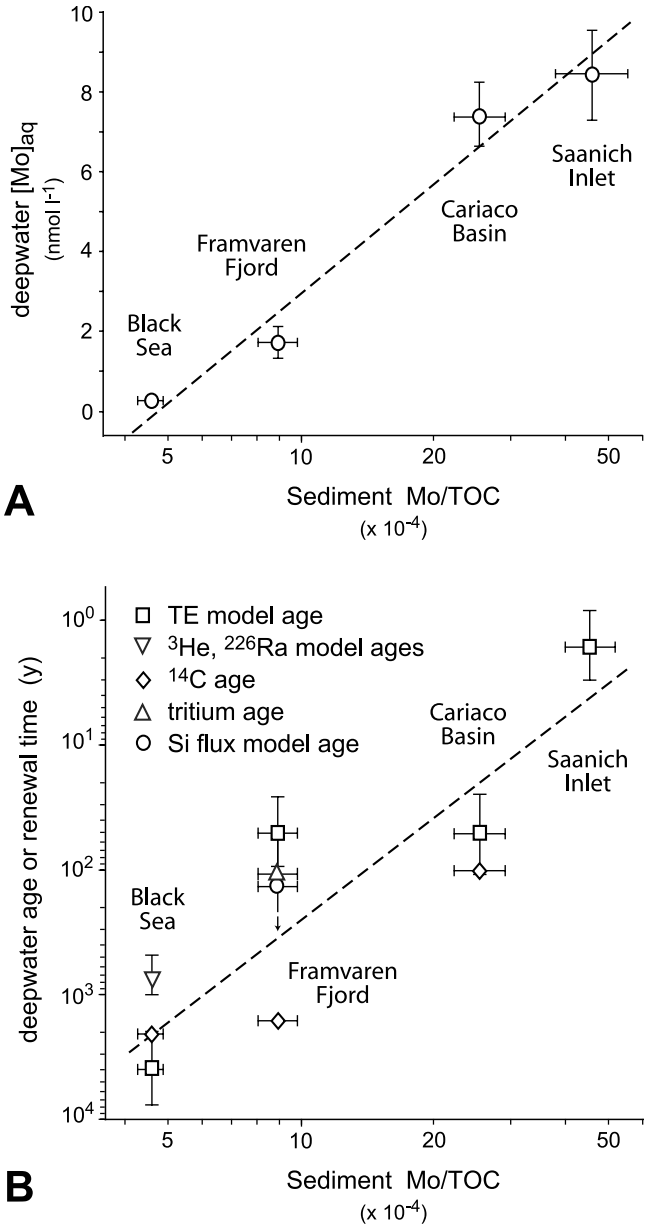

Figure 8. Sediment [Mo]/TOC versus (a) deepwater $[Mo]_{aq}$ and (b) deepwater age, τ_{dw}, for modern anoxic silled-basin environments. Correlation statistics are r^2 = 0.96, $p(\alpha)$ ~0.01 for Figure 8a and r^2 = 0.90, $p(\alpha)$ ~0.01 for Figure 8b. The ordinal scale represents the $[Mo]_s$/TOC slopes from Figure 6. Aqueous Mo concentrations are raw rather than salinity-normalized values from *Skei* [1981, 1986], *Jacobs* [1984], *Scranton et al.* [1987], and *Murray* [1991a]; deepwater ages are from *Deuser* [1973], *Östlund* [1974], *Östlund and Dyrssen* [1986], *Top et al.* [1990], *Falkner et al.* [1991], *Murray et al.* [1991], *Yao and Millero* [1995], *Dyrssen et al.* [1996], *Dyrssen* [1999], and *Shipboard Scientific Party* [1998].

average shales were taken from *Wedepohl* [1971] and *Taylor and McLennan* [1985]. Organic carbon burial fluxes were calculated as

$$f(\mathrm{OC}) = \mathrm{TOC} \times \rho_{db} \times \upsilon \times \kappa, \quad (3)$$

where f(OC) is organic carbon burial flux in g m^{-2} yr^{-1}, TOC is the concentration of sedimentary organic carbon (in%), κ is equal to 10^{-2}, and other symbols are as in equation (2). Mo and TOC burial fluxes are given on a molar and a weight basis, respectively, to conform with widely used conventions (Table 2). Mo/TOC burial flux ratios, f(Mo)/f(OC), were calculated on a common (i.e., weight) basis.

[35] Mo and TOC burial fluxes and Mo/TOC flux ratios exhibit systematic relationships to ambient environmental redox conditions, as represented by an $[O_2]_{aq}$-$[H_2S]_{aq}$ scale (Figure 7). All three variables reach maximum values under weakly sulfidic conditions (~10–50 μmol H_2S L^{-1}), peaking at ~1.1 mmol m^{-2} yr^{-1} for the Mo burial flux, ~110 g m^{-2} yr^{-1} for the TOC burial flux, and ~3.0×10^{-3} for the Mo/TOC flux ratio. From peak values in the weakly sulfidic range, Mo burial fluxes decline sharply at both higher and lower redox potentials (Figure 7a). In contrast, TOC burial fluxes decline more slowly toward higher redox potentials (i.e., more oxic conditions, Figure 7b), and Mo/TOC burial flux ratios decline more slowly toward lower redox potentials (i.e., more sulfidic conditions, Figure 7c). The latter relationship is of considerable interest for paleoenvironmental studies because the Mo/TOC burial flux ratio is equivalent to the $[Mo]_s$/TOC weight ratio of sediments, an easily measured quantity.

3. Discussion

3.1. Sedimentary Mo as a Paleohydrographic Proxy

3.1.1. Relationship to Deepwater $[Mo]_{aq}$ and Renewal Time

[36] Although many ancient black shales exhibit strong positive covariation between $[Mo]_s$ and TOC [e.g., *Holland*, 1984, pp. 485 and 493; *Robl and Barron*, 1987; *Algeo*, 2004], such relationships have received comparatively little attention and their significance is not well understood. *Algeo and Maynard* [2004] suggested that such covariation in Upper Pennsylvanian cyclothemic black shales was due to "saturation" of available sites in organic host phases by Mo and other trace metals. However, a control of this type should yield similar $[Mo]_s$/TOC ratios in all anoxic facies, which is clearly not the case for the modern anoxic marine environments considered in this study (Figure 5). Furthermore, the $[Mo]_s$/TOC ratio of a given environment can change with time, albeit slowly, as shown above for Framvaren Fjord and the Cariaco Basin (Figures 5b and 5c). These observations suggest that other, as yet unidentified, factors are responsible for Mo-TOC covariation in anoxic facies.

[37] The $[Mo]_s$/TOC ratios of the parsed sediment geochemical data sets for the present study environments exhibit strong relationships with two measures of subchemoclinal water mass restriction: deepwater $[Mo]_{aq}$ and

renewal time, τ_{dw} (Figure 8 and Table 2). The $[Mo]_s$/TOC ratios covary positively with deepwater $[Mo]_{aq}$ and negatively with τ_{dw}, with both relationships exhibiting a significance level, $p(\alpha)$, of $\sim$0.01. Positive covariation of sediment Mo/TOC ratios with deepwater $[Mo]_{aq}$ implies that the amount of Mo taken up by the sediment under anoxic conditions is dependent not only on the concentration of sedimentary organic matter (i.e., host phase availability) but also on the concentration of aqueous Mo (i.e., source ion availability):

$$[Mo]_s \equiv [TOC]_s \times [Mo]_{aq} \quad (4)$$

or

$$[Mo]_s/[TOC]_s \equiv [Mo]_{aq}, \quad (5)$$

where the subscripts s and aq denote sedimentary and aqueous, respectively. In anoxic silled basins, the rate of removal of Mo to the sediment generally exceeds the rate of resupply through deepwater renewal events. As a consequence, the Mo concentration of the deepwater mass becomes depleted, and the reduced availability of aqueous Mo is subsequently reflected in a reduced uptake of Mo by the sediment per unit organic matter. This "basin reservoir effect" is strongly linked to the degree of hydrographic restriction of the deepwater mass, which, among the present study environments, is least for Saanich Inlet and greatest for the Black Sea (e.g., Figure 3). This accounts for the systematic variation in $[Mo/TOC]_s$ ratios observed among the study environments, which range from a high of $\sim 45 \times 10^{-4}$ for Saanich Inlet to a low of $\sim 4.5 \times 10^{-4}$ for the Black Sea. Both aqueous and sedimentary Mo concentrations are linked to τ_{dw}, a direct measure of deepwater restriction, estimates of which range from a low of $\sim$1.5 years for Saanich Inlet to a high of 500–4000 years for the Black Sea.

[38] The relationships documented above provide a potential basis for assessing hydrographic conditions in ancient anoxic silled basins. This is of particular significance for paleoceanographic research because sediment Mo-TOC ratios are an easily determined quantity, whereas aqueous chemical and physical properties are not directly measurable. T. J. Algeo et al. (Hydrographic conditions of the North American Devono-Mississippian Seaway inferred from sedimentary Mo-TOC relationships, submitted to *Palaeogeography, Palaeoclimatology, Palaeoecology*, 2005) applied this approach to Devono-Carboniferous black shales deposited in silled anoxic basins of the North American cratonic interior. They determined that most of the investigated formations (42 of 48) exhibited statistically significant, positively covariant relationships between Mo and TOC, with a majority yielding correlation line slopes between 10 and 25 (units of 10^{-4}). They argued that (1) similarity of $[Mo]_s$/TOC ratios between modern and Devono-Carboniferous anoxic facies suggests similar, time-independent controls on sedimentary Mo accumulation and (2) systematic patterns of stratigraphic and geographic variation in the $[Mo]_s$/TOC ratios of Devono-Carboniferous black shales imply control by broad and slowly evolving water mass characteristics of the interior North American Seaway. On the basis of relationships documented in the present study (e.g., Figure 8), deepwater Mo concentrations for Devono-Carboniferous silled basins of the North American Seaway were estimated to be mostly between 30% and 70% of the modern seawater value, and deepwater residence times to be between $\sim$50 and $\sim$500 years. Other Phanerozoic black shales exhibiting positive Mo-TOC covariation may be amenable to this type of paleohydrographic analysis as well. An interesting question that will require further investigation is whether such techniques can be applied to anoxic facies deposited during intervals of extended global anoxia (as during much of the Precambrian) [e.g., *Anbar and Knoll*, 2002; *Arnold et al.*, 2004; *Kah et al.*, 2004], as such conditions may have resulted in wholesale drawdown of seawater trace metal inventories [e.g., *Algeo*, 2004] and produced fundamentally different sedimentary Mo-TOC relationships.

3.1.2. Relationship to Hydrographic Dynamics

[39] The hypothesis above implies that stratigraphic variation in $[Mo]_s$-TOC relationships within a single environment has the potential to yield information about the temporal dynamics of basin hydrography. This idea can be tested using high-resolution chemostratigraphic data from two of the study environments, Framvaren Fjord and the Cariaco Basin (Figures 4b and 4c). Although $[Mo]_s$-TOC covariation in these environments might appear to be random (Figures 5b and 5c), much of it can be related to historic or geologic events that influenced basin hydrography. The 46-cm-long F1 core from Framvaren Fjord, deposited during the past $\sim$250 years, contains a transition from bioturbated green muds to laminated black muds at 36 cm, representing the $\sim$1853 A.D. sill deepening event. This event resulted initially in sharp increases in both Mo and TOC (at 30–36 cm) and subsequently in a progressive shift toward higher TOC and lower Mo concentrations continuing to the present (0–30 cm, Figure 5b). Although sample-to-sample changes in $[Mo]_s$ and TOC are generally positively covariant (reflecting variation in the burial flux of organic carbon or nonorganic diluents), sediment Mo/TOC ratios exhibit a fairly steady trend toward lower values in younger sediments. This protracted shift toward lower $[Mo]_s$/TOC ratios probably reflects a decline in aqueous Mo concentrations as a result of removal to the sediment without adequate resupply through deepwater renewal (Figure 9).

[40] A similar pattern is evident in the Ocean Drilling Program Site 1002 drill core from the Cariaco Basin, in which the upper 785 cm of section records the last $\sim$15 kyr of sedimentation (Figure 4c). Here the postglacial eustatic transgression resulted in sill depths increasing from $\sim$20–45 m to the present 146 m, enhancing exchange of Cariaco Basin deepwaters with nutrient-rich intermediate waters of the Caribbean Sea and stimulating primary productivity. The onset of deepwater anoxia at $\sim$14.5 kyr B.P. resulted in the accumulation of organic-rich muds, which record initial sharp increases in sediment Mo and TOC (610–670 cm) and a subsequent trend toward higher TOC and

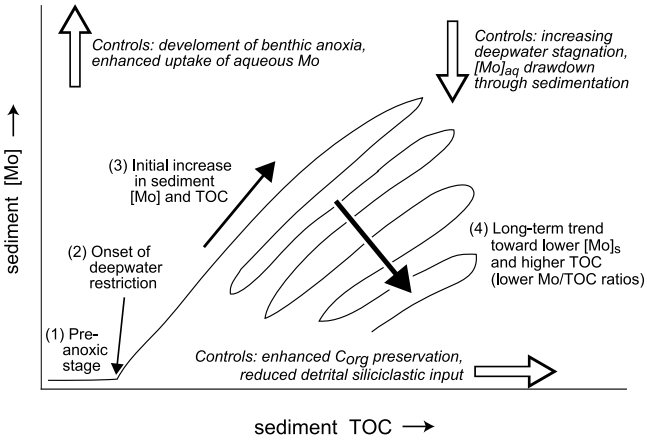

Figure 9. Generalized patterns of sedimentary Mo-TOC covariation associated with deepwater renewal in silled anoxic basins (e.g., Framvaren Fjord and Cariaco Basin) (see Figures 5b and 5c).

lower Mo concentrations (10–610 cm, Figure 5c). As for Framvaren Fjord, positive $[Mo]_s$-TOC covariation from one sample to the next reflects variation in the burial flux of organic carbon or nonorganic diluents, but the overall trend toward lower $[Mo]_s$/TOC ratios in younger sediments reflects a progressive decline in $[Mo]_{aq}$ in the deepwater mass (Figure 9).

[41] In contrast, chemostratigraphic data sets from the Black Sea and Saanich Inlet exhibit nearly constant $[Mo]_s$/TOC ratios (Figures 5a and 5d). The absence in the Black Sea cores of patterns of $[Mo]_s$-TOC covariation similar to those described above suggests that no large-scale hydrographic events have affected this silled basin during the past ~2 to 4 kyr. An interesting test of the hypothesis relating $[Mo]_s$-TOC relationships to deepwater renewal would be to generate high-resolution chemostratigraphic data for a Black Sea sediment core penetrating to at least the base of unit 2, which is ~60–80 cm below the sediment-water interface on the abyssal plain. This contact represents a major marine incursion into the Black Sea dated to ~7540 years B.P. [*Jones and Gagnon*, 1994], and one might expect to encounter in unit 2 sediments a pattern of $[Mo]_s$-TOC covariation similar to that observed in the Framvaren Fjord and Cariaco Basin cores. The lack of any significant $[Mo]_s$-TOC covariation in two Saanich Inlet cores (Figure 5d) is probably due to the diametrically opposed cause, i.e., deepwater renewal events of such high frequency (i.e., quasi-annual) that there is little chance of recording the effects of individual events in the sediment record. Mo isotopes represent another potentially useful tool for analysis of hydrographic controls on sedimentary Mo accumulation [*Barling et al.*, 2001; *Anbar*, 2004; *Arnold et al.*, 2004].

3.1.3. Significance for Mechanisms of Sedimentary Mo Enrichment

[42] Recent work has provided insight on mechanisms of sedimentary Mo enrichment. Enhanced uptake of aqueous Mo requires a critical activity of hydrogen sulfide (a_{HS^-} = $10^{-3.6}$ to $10^{-4.3}$, equivalent to ~50–250 μM HS^-), facilitating conversion of molybdate (MoO_4^{2-}) to thiomolybdates ($MoO_xS_{(4-x)}^{2-}$, x = 0 to 3) that are subsequently scavenged by sedimentary particles [*Helz et al.*, 1996; *Zheng et al.*, 2000]. Mo accumulation seems to occur primarily at or below the sediment-water interface, even in euxinic environments in which free H_2S is present in the water column [*François*, 1988; *Emerson and Huested*, 1991; *Crusius et al.*, 1996; *Zheng et al.*, 2000]. Scavenging of Mo from pore waters rather than the water column is probably due to the higher sulfide concentrations encountered below the sediment-water interface, which reflect a balance between the processes that generate H_2S (e.g., in situ sulfate reduction) and those that deplete H_2S (e.g., formation of Fe-sulfides and OM sulfurization, diffusion/advection of H_2S out of the sediment, and near-surface oxidation) [*Meyers et al.*, 2005]. Other factors that may favor Mo uptake at or below the sediment-water interface include the presence of Brønsted acids in pore waters, which promote the molybdate-to-thiomolybdate conversion, and the availability of clay mineral surfaces, which may catalyze hydrolysis and sulfidation of thiomolybdates [*Erickson and Helz*, 2000; *Vorlicek and Helz*, 2002].

[43] Some aspects of sedimentary Mo accumulation remain poorly understood, and the present study may provide some insights regarding these issues. One issue is the relative importance of various reaction paths and host phases for sedimentary Mo uptake, e.g., absorption onto humic substances [*Brumsack*, 1989; *Helz et al.*, 1996] or particulate Mn-oxyhydroxides [*Berrang and Grill*, 1974; *Magyar et al.*, 1993; *Adelson et al.*, 2001], formation of organo-metallic ligands [*Lewan and Maynard*, 1982; *Pratt and Davis*, 1992], and solid-solution uptake by authigenic sulfides [*Volkov and Fomina*, 1974; *Huerta-Diaz and Morse*, 1992; *Morse and Luther*, 1999]. Strong positive covariation between $[Mo]_s$ and TOC in modern anoxic marine environments (Figure 5) as well as in many ancient black shales [e.g., *Holland*, 1984, pp. 485 and 493; *Robl and Barron*, 1987; *Algeo*, 2004; *Algeo and Maynard*, 2004] implies that most sedimentary Mo resides in organic matter. If organic matter were not the dominant host phase, then $[Mo]_s$-TOC covariation almost certainly would be weaker and less ubiquitous. Further, scavenging of Mo by sedimentary organic matter must occur rapidly (i.e., at or close to the sediment-water interface) because strong $[Mo]_s$-TOC covariation is evident in sediments as young as a few decades (as in Framvaren Fjord, Figure 5b). Rapid uptake of Mo dominantly by organic host phases at the sediment-water interface not only is consistent with but also may represent an integral aspect of the hydrographic controls on Mo accumulation inferred above.

[44] The role of Fe-Mn redox cycling as a mechanism of Mo transfer to the sediment is incompletely understood [*Bertine and Turekian*, 1973; *Jacobs et al.*, 1985; *Emerson and Huested*, 1991; *Magyar et al.*, 1993; *Crusius et al.*, 1996; *Adelson et al.*, 2001]. Solid-phase Fe- and Mn-oxyhydroxides are known to adsorb the molybdate oxyanion in the oxic portion of the water column and transfer it to the sediment-water interface by particle sinking, where it is released through reductive dissolution and either diffuses back into the water column or is scavenged by other phases within the sediment.

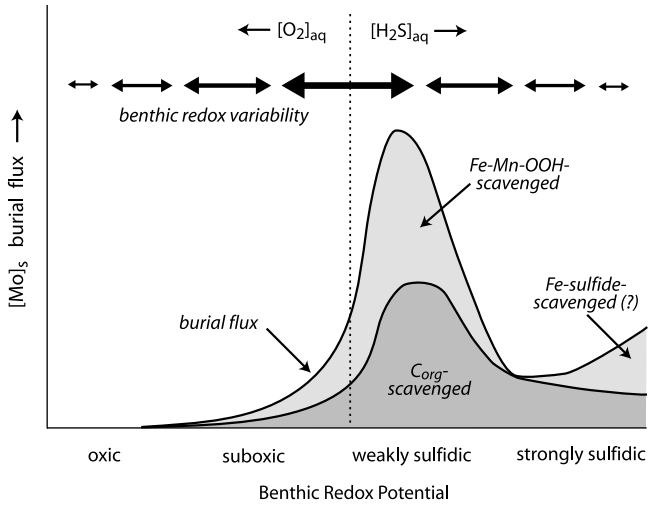

Figure 10. Model of dominant controls on Mo burial fluxes as a function of benthic redox potential. Under oxic conditions, little aqueous Mo is scavenged. With decreasing redox potential (toward the right), Mo burial fluxes increase to a peak in the weakly sulfidic range. Contributing to this peak is accelerated transfer to the sediment of molybdate adsorbed onto Fe-Mn-oxyhydroxides and direct scavenging of thiomolybdates by organic matter at the sediment-water interface. Under strongly sulfidic and non-Fe-limiting conditions, Mo uptake in solid solution by authigenic Fe-sulfides, either in the water column or at the sediment-water interface, may become important. At top, arrow size gives schematically the scale of local redox variation as a function of benthic redox potential.

Scavenging of released Mo by organic matter is likely to contribute to Mo enrichment and $[Mo]_s$-TOC covariation in the sediment (see above). The importance of Fe-Mn redox cycling for sedimentary Mo accumulation appears to be strongly redox-dependent. In environments with persistently sulfidic deepwaters (e.g., the Black Sea and Framvaren Fjord), Fe-Mn redox cycling occurs entirely within the water column with little or no adsorbed Mo reaching the sediment-water interface [*Jacobs et al.*, 1985; *Skei et al.*, 1996; *Crusius et al.*, 1996]. In contrast, in environments with suboxic to weakly sulfidic deepwaters, especially those subject to redox variations at short (e.g., seasonal) timescales, Fe-Mn redox cycling may be a major factor enhancing Mo transfer to the sediment [*Murray*, 1975; *Crusius et al.*, 1996]. In such settings, vertical fluctuations of the O_2-H_2S redox boundary alternately promote (1) Mo scavenging in the water column as the chemocline recedes below the sediment-water interface and oxidizing (albeit suboxic) deepwaters catalyze precipitation of solid-phase Fe-Mn-oxyhydroxides and (2) Mo release at the sediment-water interface as the chemocline rises into the water column and sulfidic bottom waters catalyze reductive dissolution of Fe-Mn-oxyhydroxides in surficial sediments. This process represents a "Mo pump" that may be responsible for the exceptionally large Mo burial fluxes (Figure 7a) and intermittently high Mo concentrations in sediment traps at Saanich Inlet [*Berrang and Grill*, 1974; *François*, 1988]. Enhanced Mo uptake through Fe-Mn redox cycling is consistent with the hydrographic controls on sedimentary Mo accumulation inferred above.

[45] Authigenic Fe-sulfide precipitation has been proposed as an important vector of sedimentary Mo uptake [e.g., *Piper and Isaacs*, 1996]. Positive $[Mo]_s$-TOC covariation is not necessarily inconsistent with authigenic Fe-sulfides as a major host phase for sedimentary Mo, if higher rates of bacterial sulfate reduction and H_2S generation were associated with higher organic C burial fluxes [e.g., *Dean et al.*, 1999]. However, several considerations argue against a major role for Fe-sulfides in Mo accumulation in most anoxic depositional systems. First, $[Mo]_s$ rarely shows significant covariation with pyrite S or total S concentrations in sediments [*Lyons et al.*, 2003; *Algeo and Maynard*, 2004]. Second, Mo burial fluxes are inversely related to deepwater $[H_2S]_{aq}$ in modern anoxic silled basins (Figure 7a), a consequence of drawdown of deepwater $[Mo]_{aq}$ under more stagnant conditions (i.e., the "basin reservoir effect"). Thus, although small quantities of Mo are demonstrably present in solid solution in Fe-sulfides [e.g., *Huerta-Diaz and Morse*, 1992; *Morse and Luther*, 1999], there is no evidence that this represents a major vector of Mo transfer to the sediment in anoxic depositional systems.

3.2. Sedimentary Mo as a Paleoredox Proxy

[46] Sedimentary Mo data have been widely employed as a paleoredox proxy, with higher concentrations interpreted to reflect lower redox potentials (as measured on an $[O_2]$-$[H_2S]$ continuum such as in Figure 10) [e.g., *Emerson and Huested*, 1991; *Piper*, 1994; *Jones and Manning*, 1994; *Crusius et al.*, 1996; *Dean et al.*, 1997, 1999; *Morford and Emerson*, 1999; *Piper and Dean*, 2002; *Lyons et al.*, 2003; *Sageman et al.*, 2003; *Algeo and Maynard*, 2004]. Although anoxic facies are almost invariably enriched in Mo relative to oxic and suboxic facies, it is unclear whether sedimentary Mo concentrations or burial fluxes exhibit a systematic relationship to benthic redox potential within euxinic environments. If Mo scavenging by authigenic Fe-sulfides is quantitatively important and sulfide formation is not severely Fe-limited, then one might expect negative covariation between sedimentary Mo and benthic redox potential (i.e., higher Mo concentrations and burial fluxes under more strongly sulfidic conditions) [e.g., *Algeo and Maynard*, 2004]. If, on the other hand, H_2S concentrations influence sedimentary Mo accumulation only by serving as a "geochemical switch" with a specific activation point [e.g., *Helz et al.*, 1996], then one might predict little relationship between $[Mo]_s$ and benthic redox potential. In fact, the dominant relationship documented in the present study of modern anoxic silled basins is positive covariation between sedimentary Mo and benthic redox potential (i.e., lower Mo concentrations and burial fluxes at higher aqueous sulfide concentrations).

[47] Positive covariation between sedimentary Mo and benthic redox potential is manifested in several ways. First, Mo burial fluxes peak under weakly reducing conditions

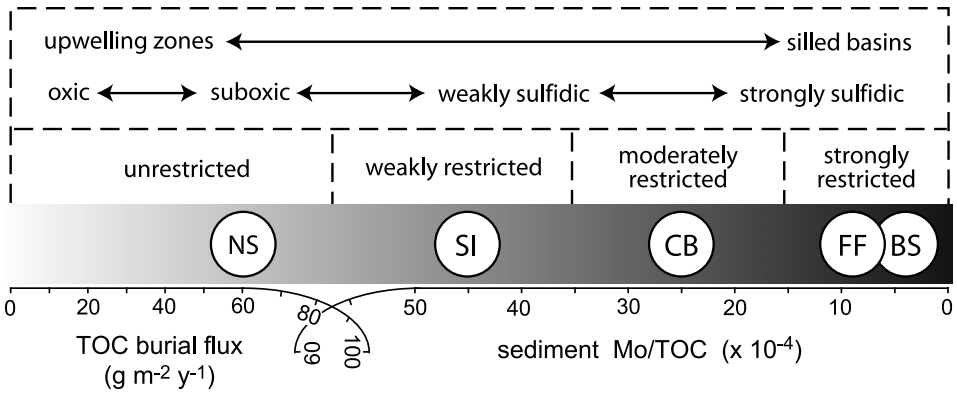

Figure 11. Environmental scale for anoxic marine environments based on degree of hydrographic restriction and benthic redox potential. Abbreviations for modern environments are NS, Namibian Shelf; SI, Saanich Inlet; CB, Cariaco Basin; FF, Framvaren Fjord; and BS, Black Sea. See text for details of scale construction.

($\sim$10–50 μmol H_2S L^{-1}) and decrease at higher H_2S concentrations (Figures 6 and 10). Second, within individual anoxic silled basins, large-scale deepwater renewal tends to produce an initial rapid increase in sedimentary Mo concentrations followed by a long-term trend toward lower $[Mo]_s$ and higher TOC values (Figure 9, compare Figures 5b and 5c). Third, the amount of sedimentary Mo accumulated per unit organic carbon, $[Mo]_s$/TOC, decreases with increasing restriction of the subpycnoclinal water mass, as proxied by deepwater $[Mo]_{aq}$ or τ_{dw} (Figure 8). The first relationship is interpreted to represent enhanced transfer of Mo to the sediment under weakly sulfidic and highly dynamic benthic redox conditions, possibly associated with intense Fe-Mn redox cycling within the water column (as in Saanich Inlet, Figure 10). The second relationship is interpreted to represent drawdown of aqueous Mo concentrations in silled anoxic basins owing to rates of Mo removal to the sediment in excess of resupply during the stagnant intervals between deepwater renewal events (i.e., the "basin reservoir effect," Figure 9). The third relationship is due to a combination of these two processes. Thus sedimentary Mo concentrations and burial fluxes generally tend to decrease as the bottom waters of silled euxinic basins become more reducing (i.e., sulfide-rich).

3.3. Environments of Application of the Sedimentary Mo Proxy

[48] It should be emphasized that the relationships documented above (linking sediment and water mass Mo concentrations, Figure 8) are applicable only to anoxic facies subject to some degree of hydrographic restriction (e.g., silled basins) and are almost certainly not valid for anoxic facies in open marine settings where hydrographic restriction is limited or nonexistent (e.g., continent-margin upwelling systems). This point is illustrated by the Namibian Shelf, a modern upwelling system with a $[Mo]_s$/TOC ratio of $\sim$6 $\pm$ 3, reflecting relatively limited uptake of sedimentary Mo per unit organic matter (Figure 5e). Given the ready availability of aqueous Mo in undepleted seawater and rapid turnover of the deepwater mass on the Namibian Shelf, this low $[Mo]_s$/TOC ratio cannot be understood in terms of hydrographic controls. Rather, limited Mo uptake in open marine anoxic facies is probably due to aqueous H_2S concentrations at the sediment-water interface being below the critical threshold for conversion of molybdate to thiomolybdate most of the time [*Helz et al.*, 1996]. This limitation may be a general feature of upwelling systems, i.e., water mass exchange that is sufficiently rapid to prevent buildup in the water column of $[H_2S]$ diffusing out of the sediment to any significant degree. Although sediments accumulating on the Namibian Shelf (and in other modern upwelling zones) are organic-rich, they record mainly suboxic to anoxic nonsulfidic seafloor conditions [e.g., *Piper and Isaacs*, 1996]. Differences in the relationships of Mo and TOC burial fluxes to benthic redox potential (Figure 7) demonstrate the potential for accumulation of large quantities of organic matter with only limited Mo uptake by sediments if redox conditions are persistently in the suboxic range.

[49] The relationships documented above also have important implications for the use of sedimentary Mo as a paleoredox proxy. Strong control of sedimentary Mo uptake by hydrographic factors in restricted anoxic environments results in lack of a systematic relationship between $[Mo]_s$ and benthic redox potential. If any relationship exists, it is a counterintuitive one in which Mo burial fluxes and $[Mo]_s$/TOC ratios decrease as redox conditions become increasingly sulfidic (e.g., Figure 7). For this reason, sedimentary Mo concentrations cannot be used to infer redox variation (i.e., variable sulfide concentrations) within restricted marine environments. This inference is in no way inconsistent with the observation that anoxic facies are generally enriched in sedimentary Mo relative to oxic and suboxic facies. Further, it does not exclude the possibility that sedimentary Mo concentrations may generally increase as redox conditions become more sulfidic in unrestricted anoxic marine environments, e.g., upwelling systems such as the Namibian Shelf (Figure 10). In such environments, sedimentary Mo uptake is unlikely to be influenced by hydrographic factors, and, consequently, other controls such as benthic redox potential may become dominant. The results of this study suggest that application

of sedimentary Mo as a paleoredox proxy must be undertaken cautiously and with due consideration given to the relationships documented above. In general, use of $[Mo]_s$ as a paleoredox proxy needs to be justified through (1) hydrographic analysis of the paleoenvironment of interest, i.e., assessment of basinal configuration, circulation patterns, and other factors influencing the aqueous chemistry and degree of restriction of the subpycnoclinal water mass, and (2) comparison with other, independent paleoredox proxies.

3.4. Significance for Classification of Anoxic Environments

[50] Existing classifications of anoxic marine environments consist of a number of discrete models based on conceptualized geographic and hydrographic conditions [e.g., *Demaison and Moore*, 1980; *Arthur and Sageman*, 1994; *Wignall*, 1994]. These schemes generally offer few quantitative measures by which to evaluate the environmental characteristics of ancient anoxic marine systems and their "goodness of fit" to existing models. The results of the present study suggest a new approach to assessment of anoxic paleoenvironments, one based on paleoenvironmental parameters that can be estimated from measurable, objective criteria. An important variable in anoxic depositional systems is the degree of restriction of the subchemoclinal water mass, which influences many aspects of its aqueous chemistry including deepwater $[H_2S]_{aq}$, $[Mo]_{aq}$, and age (Table 2 and Figures 2 and 3). Sedimentary Mo-TOC data can provide a framework for analysis and classification of anoxic paleoenvironments on this basis (Figure 11). As shown above, $[Mo]_s$/TOC ratios are useful for distinguishing degrees of restriction of the subchemoclinal water mass in anoxic marine environments, with values of >35, ~15–35, and <15($\times 10^{-4}$) associated with weak, moderate, and strong restriction, respectively. Benthic redox potential also varies systematically along this hydrographic continuum, with fluctuating, suboxic to weakly sulfidic conditions associated with weakly restricted basins and stable, strongly sulfidic conditions associated with strongly restricted basins (Figures 10 and 11). Recognition of the continuity of water mass restriction, and of the chemical attributes that define it, significantly increases the utility of modern anoxic marine environments as analogs for oxygen-deficient paleoenvironments, even when the boundary conditions of the latter do not exactly match those of any modern anoxic marine system.

4. Conclusions

[51] Although Mo is enriched in anoxic facies relative to oxic and suboxic facies, there is no systematic relationship between $[Mo]_s$ and dissolved sulfide concentrations within euxinic marine environments. Rather, sedimentary Mo concentrations are controlled mainly by the degree of water mass restriction in modern anoxic silled basins. As the degree of restriction increases, the amount of Mo taken up by the sediment per unit organic carbon, $[Mo]_s$/TOC, decreases, a consequence of drawdown of deepwater $[Mo]_{aq}$ through removal to the sediment without adequate resupply by deepwater renewal. In moving from weakly restricted silled basins such as Saanich Inlet (τ_{dw} < 2 years) to strongly restricted silled basins such as the Black Sea (τ_{dw} > 500 years), deepwater $[Mo]_{aq}$ declines from ~100% to <5% of the seawater value and $[Mo]_s$/TOC ratios decline from $45 \pm 5 \times 10^{-4}$ to $4.5 \pm 1 \times 10^{-4}$. Strong correlations among aqueous and sedimentary variables related to water mass restriction in modern anoxic silled basins suggest that the $[Mo]_s$/TOC ratios of ancient black shales can be used to estimate the deepwater $[Mo]_{aq}$ and age of restricted anoxic paleoenvironments. However, these relationships cannot be applied to anoxic facies in open marine settings, e.g., continent-margin upwelling systems such as the Namibian Shelf, in which water mass exchange is unrestricted. The dominant vectors of Mo transfer to the sediment are probably redox-dependent: Mo burial fluxes peak in weakly sulfidic facies owing to greater aqueous Mo availability and to enhanced scavenging associated with Fe-Mn cycling, whereas Mo removal to the sediment decreases in strongly sulfidic facies as a result of the reduced availability of aqueous Mo in highly restricted water masses. Analysis and classification of anoxic paleoenvironments may benefit from application of quantifiable sedimentary proxies for scalable environmental variables (e.g., $[Mo]_s$/TOC ratios as a proxy for degree of hydrographic restriction).

[52] **Acknowledgments.** Thanks go to Tim Phillips for drafting assistance, to Clint Scott and Ben Gill for helpful discussions, and to Ariel Anbar and an anonymous reviewer for reviews of the manuscript. This study was supported in part by grants from the University of Cincinnati Research Council (T.J.A.) and the U.S. National Science Foundation (EAR-9875961 and EAR-0230097) and the NASA Exobiology Program (T.W.L.).

References

Adelson, J. M., G. R. Helz, and C. V. Miller (2001), Reconstructing the rise of recent coastal anoxia: Molybdenum in Chesapeake Bay sediments, *Geochim. Cosmochim. Acta*, *65*, 237–252.

Algeo, T. J. (2004), Can marine anoxic events draw down the trace-element inventory of seawater?, *Geology*, *32*, 1057–1060.

Algeo, T. J., and J. B. Maynard (2004), Trace element behavior and redox facies in core shales of Upper Pennsylvanian Kansas-type cyclothems, *Chem. Geol.*, *206*, 289–318.

Algeo, T. J., L. Schwark, and J. C. Hower (2004), High-resolution geochemistry and sequence stratigraphy of the Hushpuckney Shale (Swope Formation, eastern Kansas): Implications for climato-environmental dynamics of the Late Pennsylvanian Midcontinent Seaway, *Chem. Geol.*, *206*, 259–288.

Anbar, A. D. (2004), Molybdenum stable isotopes: Observations, interpretations and directions, in *Geochemistry of Non-Traditional Stable Isotopes*, edited by C. Johnson et al., *Rev. Mineral. Geochem.*, vol. 55, pp. 429–454, Mineral. Soc. of Am., Washington, D. C.

Anbar, A. D., and A. H. Knoll (2002), Proterozoic ocean chemistry and evolution: A bioinorganic bridge?, *Science*, *297*, 1137–1142.

Anderson, J. J., and A. H. Devol (1973), Deep water renewal in Saanich Inlet, an intermittently anoxic basin, *Estuarine Coastal Mar. Sci.*, *1*, 1–10.

Anderson, L. G., D. Dyrssen, and P. O. J. Hall (1988), On the sulphur chemistry of a super-

anoxic fjord, Framvaren, south Norway, *Mar. Chem.*, *23*, 283–293.
Anderson, R. F., and M. Q. Fleisher (1991), Uranium precipitation in Black Sea sediments, in *Black Sea Oceanography*, edited by E. Izdar and J. W. Murray, pp. 443–458, Springer, New York.
Anderson, R. F., T. W. Lyons, and G. L. Cowie (1994), Sedimentary record of a shoaling of the oxic/anoxic interface in the Black Sea, *Mar. Geol.*, *116*, 373–384.
Arnold, G. L., A. D. Anbar, J. Barling, and T. W. Lyons (2004), Molybdenum isotope evidence for widespread anoxia in mid-Proterozoic oceans, *Science*, *304*, 87–90.
Arthur, M. A., and B. B. Sageman (1994), Marine black shales: Depositional mechanisms and environments of ancient deposits, *Annu. Rev. Earth Planet. Sci.*, *22*, 499–551.
Arthur, M. A., W. E. Dean, E. D. Neff, B. J. Hay, J. King, and G. Jones (1994), Varve-calibrated records of carbonate and organic carbon accumulation over the last 2000 years in the Black Sea, *Global Biogeochem. Cycles*, *8*, 195–217.
Barling, J., G. L. Arnold, and A. D. Anbar (2001), Natural mass-dependent variations in the isotopic composition of molybdenum, *Earth Planet. Sci. Lett.*, *193*, 447–457.
Berrang, P. G., and E. V. Grill (1974), The effect of manganese oxide scavenging on molybdenum in Saanich Inlet, British Columbia, *Mar. Chem.*, *2*, 125–148.
Bertine, K. K., and K. K. Turekian (1973), Molybdenum in marine deposits, *Geochim. Cosmochim. Acta*, *37*, 1415–1434.
Bremner, J. M. (1983), Biogenic sediments on the south West African (Namibian) continental margin, in *Coastal Upwelling: Its Sediment Record*, part B, *Sedimentary Records of Ancient Coastal Upwelling*, edited by J. Thiede and E. Suess, pp. 73–103, Springer, New York.
Brewer, P. G., and D. W. Spencer (1974), Distribution of some trace elements in Black Sea and their flux between dissolved and particulate phases, in *The Black Sea—Geology, Chemistry, and Biology*, edited by E. T. Degens and D. A. Ross, *AAPG Mem.*, *20*, 137–143.
Brongersma-Sanders, M., K. M. Stephan, T. G. Kwee, and M. De Bruin (1980), Distribution of minor elements in cores from the southwest Africa shelf with notes on plankton and fish mortality, *Mar. Geol.*, *37*, 91–132.
Brumsack, H. J. (1989), Geochemistry of recent TOC-rich sediments from the Gulf of California and the Black Sea, *Geol. Rundsch.*, *78*, 851–882.
Calvert, S. E., and N. B. Price (1970), Minor metal contents of Recent organic-rich sediments off south west Africa, *Nature*, *227*, 593–595.
Calvert, S. E., and N. B. Price (1983), Geochemistry of Namibian Shelf sediments, in *Coastal Upwelling: Its Sediment Record*, part A, *Responses of the Sedimentary Regime to Present Coastal Upwelling*, edited by E. Suess and J. Thiede, pp. 337–375, Springer, New York.
Calvert, S. E., R. E. Karlin, L. J. Toolin, D. J. Donahue, J. R. Southon, and J. S. Vogel (1991), Low organic carbon accumulation rates in Black Sea sediments, *Nature*, *350*, 692–695.
Chapman, P., and G. W. Bailey (1991), Short-term variability during an anchor station study in the southern Benguela upwelling system: Introduction, *Prog. Oceanogr.*, *28*, 1–7.
Chapman, P., and L. V. Shannon (1985), Seasonality in the oxygen minimum layers at the extremities of the Benguela system, *S. Afr. J. Mar. Sci.*, *5*, 85–94.
Colodner, D., J. Edmond, and E. Boyle (1995), Rhenium in the Black Sea: Comparison with molybdenum and uranium, *Earth Planet. Sci. Lett.*, *131*, 1–15.
Crusius, J., S. Calvert, T. Pedersen, and D. Sage (1996), Rhenium and molybdenum enrichments in sediments as indicators of oxic, suboxic and sulfidic conditions of deposition, *Earth Planet. Sci. Lett.*, *145*, 65–78.
Crusius, J., T. F. Pedersen, S. E. Calvert, G. L. Cowie, and T. Oba (1999), A 35 kyr geochemical record from the Sea of Japan of organic matter flux variations and changes in intermediate water oxygen concentrations, *Paleoceanography*, *14*, 248–259.
Dean, W. E., J. V. Gardner, and D. Z. Piper (1997), Inorganic geochemical indicators of glacial-interglacial changes in productivity and anoxia of the California continental margin, *Geochim. Cosmochim. Acta*, *61*, 4507–4518.
Dean, W. E., D. Z. Piper, and L. C. Peterson (1999), Molybdenum accumulation in Cariaco basin sediment over the past 24 k. y.: A record of water-column anoxia and climate, *Geology*, *27*, 507–510.
Degens, E. T., and D. A. Ross (Eds.) (1974), *The Black Sea—Geology, Chemistry, and Biology*, *AAPG Mem.*, *20*, 633 pp.
Demaison, G. J., and G. T. Moore (1980), Anoxic environments and oil source bed genesis, *AAPG Bull.*, *64*, 1179–1209.
Deuser, W. G. (1973), Cariaco Trench—Oxidation of organic matter and residence time of anoxic water, *Nature*, *242*, 601–603.
Dingle, R. V., and G. Nelson (1993), Sea-bottom temperature, salinity and dissolved oxygen on the continental margin off south-western Africa, *S. Afr. J. Mar. Sci.*, *13*, 33–49.
Dyrssen, D. W. (1999), Framvaren and the Black Sea—Similarities and differences, *Aquat. Geochem.*, *5*, 59–73.
Dyrssen, D. W., P. O. J. Hall, C. Haraldsson, M. Chierici, J. Skei, and H. G. Östlund (1996), Time dependence of organic matter decay and mixing processes in Framvaren, a permanently anoxic fjord in south Norway, *Aquat. Geochem.*, *2*, 111–129.
Emerson, S. R., and S. S. Huested (1991), Ocean anoxia and the concentrations of molybdenum and vanadium in seawater, *Mar. Chem.*, *34*, 177–196.
Erickson, B. E., and G. R. Helz (2000), Molybdenum(VI) speciation in sulfidic waters: Stability and lability of thiomolybdates, *Geochim. Cosmochim. Acta*, *64*, 1149–1158.
Falkner, K. K., D. J. O'Neill, J. F. Todd, W. S. Moore, and J. M. Edmond (1991), Depletion of barium and radium-226 in Black Sea surface waters over the past thirty years, *Nature*, *350*, 491–494.
François, R. (1987), Some aspects of the geochemistry of sulphur and iodine in marine humic substances and transition metal enrichment in anoxic sediments, Ph.D. dissertation, 462 pp., Univ. of B. C., Vancouver, B.C., Canada.
François, R. (1988), A study on the regulation of the concentrations of some trace metals (Rb, Sr, Zn, Pb, Cu, V, Cr, Ni, Mn and Mo) in Saanich Inlet sediments, British Columbia, Canada, *Mar. Geol.*, *83*, 285–308.
Friedrich, H. J., and E. V. Stanev (1989), Parameterization of vertical diffusion in a numerical model of the Black Sea, in *Small-Scale Turbulence and Mixing in the Ocean*, edited by J. C. J. Nihoul and B. M. Jamart, pp. 151–167, Elsevier, New York.
Fry, B., H. W. Jannasch, S. J. Molyneaux, C. O. Wirsen, J. A. Muramoto, and S. King (1991), Stable isotope studies of the carbon, nitrogen and sulfur cycles in the Black Sea and Cariaco Trench, *Deep Sea Res., Part A*, *38*, S1003–S1019.
Gade, H. G., and A. Edwards (1980), Deep-water renewal in fjords, in *Fjord Oceanography*, edited by H. J. Freeland et al., pp. 453–489, Plenum, New York.
Gunnerson, C. G., and E. Özturgut (1974), The Bosporus, in *The Black Sea—Geology, Chemistry, and Biology*, edited by E. T. Degens and D. A. Ross, *AAPG Mem.*, *20*, 99–114.
Haug, G. H., T. F. Pedersen, D. M. Sigman, S. E. Calvert, B. Nielsen, and L. C. Peterson (1998), Glacial/interglacial variations in production and nitrogen fixation in the Cariaco Basin during the last 580 kyr, *Paleoceanography*, *13*, 427–432.
Helz, G. R., C. V. Miller, J. M. Charnock, J. F. W. Mosselmans, R. A. D. Pattrick, C. D. Garner, and D. J. Vaughan (1996), Mechanism of molybdenum removal from the sea and its concentration in black shales: EXAFS evidence, *Geochim. Cosmochim. Acta*, *60*, 3631–3642.
Hirst, D. M. (1974), Geochemistry of sediments from eleven Black Sea cores, in *The Black Sea—Geology, Chemistry, and Biology*, edited by E. T. Degens, and D. A. Ross, *AAPG Mem.*, *20*, 430–455.
Holland, H. D. (1984), *The Chemical Evolution of the Atmosphere and Oceans*, 582 pp., Princeton Univ. Press, Princeton, N. J.
Holmen, K. J., and C. G. H. Rooth (1990), Ventilation of the Cariaco Trench, a case of multiple source competition?, *Deep Sea Res., Part A*, *37*, 203–225.
Huerta-Diaz, M. G., and J. W. Morse (1992), Pyritization of trace metals in anoxic marine sediments, *Geochim. Cosmochim. Acta*, *56*, 2681–2702.
Hughen, K. A., J. T. Overpeck, S. J. Lehman, M. Kashgarian, J. Southon, L. C. Petersonk, R. Alley, and D. M. Sigman (1998), Deglacial changes in ocean circulation from an extended radiocarbon calibration, *Nature*, *391*, 65–68.
Jacobs, L. A. (1984), Metal geochemistry in anoxic marine basins, Ph.D. dissertation, 217 pp., Univ. of Wash., Seattle.
Jacobs, L., S. Emerson, and J. Skei (1985), Partitioning and transport of metals across the O_2/H_2S interface in a permanently anoxic basin: Framvaren Fjord, Norway, *Geochim. Cosmochim. Acta*, *49*, 1433–1444.
Jacobs, L., S. Emerson, and S. S. Huested (1987), Trace metal geochemistry in the Cariaco Trench, *Deep Sea Res., Part A*, *34*, 965–981.
Jones, B., and D. A. C. Manning (1994), Comparison of geochemical indices used for the interpretation of palaeoredox conditions in ancient mudstones, *Chem. Geol.*, *111*, 111–129.
Jones, G. A., and A. R. Gagnon (1994), Radiocarbon chronology of Black Sea sediments, *Deep Sea Res., Part A*, *41*, 531–557.
Kah, L. C., T. D. Frank, and T. W. Lyons (2004), Low marine sulphate and protracted oxygenation of the Proterozoic biosphere, *Nature*, *431*, 834–838.
Karl, D. M., and G. A. Knauer (1991), Microbial production and particle flux in the upper 350 m

of the Black Sea, *Deep Sea Res., Part A*, *38*, S921–S942.
Landing, W. M., and S. Westerlund (1988), The solution chemistry of iron(II) in Framvaren Fjord, *Mar. Chem.*, *23*, 329–343.
Lewan, M. D., and J. B. Maynard (1982), Factors controlling the enrichment of vanadium and nickel in the bitumen of organic sedimentary rocks, *Geochim. Cosmochim. Acta*, *46*, 2547–2560.
Lyons, T. W. (1991), Upper Holocene sediments of the Black Sea: Summary of Leg 4 box cores (1988 Black Sea Oceanographic Expedition), in *Black Sea Oceanography*, edited by E. Izdar and J. W. Murray, pp. 401–441, Springer, New York.
Lyons, T. W. (1992), Comparative study of Holocene Black Sea sediments from oxic and anoxic sites of deposition: Geochemical and sedimentological criteria, Ph.D. dissertation, 377 pp., Yale Univ., New Haven, Conn.
Lyons, T. W. (1997), Sulfur isotopic trends and pathways of iron sulfide formation in upper Holocene sediments of the anoxic Black Sea, *Geochim. Cosmochim. Acta*, *61*, 3367–3382.
Lyons, T. W., and R. A. Berner (1992), Carbon-sulfur-iron systematics of the uppermost deep-water sediments of the Black Sea, *Chem. Geol.*, *99*, 1–27.
Lyons, T. W., R. A. Berner, and R. F. Anderson (1993), Evidence for large pre-industrial perturbations of the Black Sea chemocline, *Nature*, *365*, 538–540.
Lyons, T. W., J. P. Werne, D. J. Hollander, and R. W. Murray (2003), Contrasting sulfur geochemistry and Fe/Al and Mo/Al ratios across the last oxic-to-anoxic transition in the Cariaco Basin, Venezuela, *Chem. Geol.*, *195*, 131–157.
Magyar, B., H. C. Moor, and L. Sigg (1993), Vertical distribution and transport of molybdenum in a lake with a seasonally anoxic hypolimnion, *Limnol. Oceanogr.*, *38*, 521–531.
Matthäus, W. (1995), Natural variability and human impacts reflected in long-term changes in the Baltic deep-water conditions—A brief review, *Dtsch. Hydrogr. Z.*, *47*, 47–65.
Meyers, S. R., B. B. Sageman, and T. W. Lyons (2005), Organic carbon burial rate and the molybdenum proxy: Theoretical framework and application to Cenomanian-Turonian oceanic anoxic event 2, *Paleoceanography*, *20*, PA2002, doi:10.1029/2004PA001068.
Millero, F. J. (1996), *Chemical Oceanography*, 2nd ed., 469 pp., CRC Press, Boca Raton, Fla.
Molvaer, J. (1980), Deep-water renewals in the Frierfjord—An intermittently anoxic basin, in *Fjord Oceanography*, edited by H. J. Freeland et al., pp. 531–539, Springer, New York.
Morford, J. L., and S. Emerson (1999), The geochemistry of redox sensitive trace metals in sediments, *Geochim. Cosmochim. Acta*, *63*, 1735–1750.
Morford, J. L., A. D. Russell, and S. Emerson (2001), Trace metal evidence for changes in the redox environment associated with the transition from terrigenous clay to diatomaceous sediment, Saanlich Inlet, BC, *Mar. Geol.*, *174*, 355–369.
Morse, J. W., and G. W. Luther III (1999), Chemical influences on trace metal-sulfide interactions in anoxic sediments, *Geochim. Cosmochim. Acta*, *63*, 3373–3378.
Müller-Karger, F., et al. (2001), Annual cycle of primary productivity in the Cariaco Basin—Response to upwelling and implications for vertical export, *J. Geophys. Res.*, *106*, 4527–4542.
Murray, J. W. (1975), The interaction of metal ions at the manganese dioxide-solution interface, *Geochim. Cosmochim. Acta*, *42*, 1011–1026.
Murray, J. W. (1991a), Hydrographic variability in the Black Sea, in *Black Sea Oceanography*, edited by E. Izdar and J. W. Murray, pp. 1–15, Springer, New York.
Murray, J. W. (Ed.) (1991b), Black Sea oceanography: Results of the 1988 Black Sea expedition, *Deep Sea Res., Part A*, *38*, S655–S1266.
Murray, J. W., H. W. Jannasch, S. Honjo, R. F. Anderson, W. S. Reeburgh, Z. Top, G. E. Friederich, L. A. Codispoti, and E. Izdar (1989), Unexpected changes in the oxic/anoxic interface in the Black Sea, *Nature*, *338*, 411–413.
Murray, J. W., Z. Top, and E. Oszoy (1991), Hydrographic properties and ventilation of the Black Sea, *Deep Sea Res., Part A*, *38*, S663–S689.
Naes, K., J. M. Skei, and P. Wassmann (1988), Total particulate and organic fluxes in anoxic Framvaren waters, *Mar. Chem.*, *23*, 257–268.
Östlund, H. G. (1974), Expedition "Odysseus 65": Radiocarbon age of Black Sea deep water, in *The Black Sea—Geology, Chemistry, and Biology*, edited by E. T. Degens and D. A. Ross, *AAPG Mem.*, *20*, 127–132.
Östlund, H. G., and D. Dyrssen (1986), Renewal rates of the Black Sea deep water, in *The Chemical and Physical Oceanography of the Black Sea*, *Rep. Chem. Sea XXXIII*, Univ. of Göteborg, Göteborg, Sweden.
Peterson, L. C., J. T. Overpeck, N. G. Kipp, and J. Imbrie (1991), A high-resolution late Quaternary upwelling record from the anoxic Cariaco Basin, Venezuela, *Paleoceanography*, *6*, 99–119.
Peterson, L. C., G. H. Haug, R. W. Murray, K. M. Yarincik, J. W. King, T. J. Bralower, K. Kameo, S. D. Rutherford, and R. B. Pearce (2000), Late Quaternary stratigraphy and sedimentation at Site 1002, Cariaco Basin (Venezuela), in *Proc. Ocean Drill. Program Sci. Results*, *165*, 85–99.
Piper, D. Z. (1994), Seawater as the source of minor elements in black shales, phosphorites, and other sedimentary deposits, *Chem. Geol.*, *114*, 95–114.
Piper, D. Z., and W. E. Dean (2002), Trace-element deposition in the Cariaco Basin, Venezuela Shelf, under sulfate-reducing conditions—A history of the local hydrography and global climate, 20 ka to the present, *U.S. Geol. Surv. Prof. Pap.*, *1670*, 41 pp.
Piper, D. Z., and C. M. Isaacs (1996), Instability of bottom-water redox conditions during accumulation of Quaternary sediments in the Japan Sea, *Paleoceanography*, *11*, 171–190.
Popescu, I., G. Lericolais, N. Panin, A. Normand, C. Dinu, and E. Le Drezen (2004), The Danube submarine canyon (Black Sea): Morphology and sedimentary processes, *Mar. Geol.*, *206*, 249–265.
Pratt, L. M., and C. L. Davis (1992), Intertwined fates of metals, sulfur, and organic carbon in black shales, in *Geochemistry of Organic Matter in Sediments and Sedimentary Rocks*, edited by L. M. Pratt et al., *SEPM Short Course*, *27*, 1–27.
Price, N. B., and S. E. Calvert (1973), The geochemistry of iodine in oxidized and reduced Recent marine sediments, *Geochim. Cosmochim. Acta*, *37*, 2149–2158.
Ravizza, G., K. K. Turekian, and B. J. Hay (1991), The geochemistry of rhenium and osmium in recent sediments from the Black Sea, *Geochim. Cosmochim. Acta*, *55*, 3741–3752.
Robl, T. L., and L. S. Barron (1987), The geochemistry of Devonian black shales in central Kentucky and its relationship to interbasinal correlation and depositional environment, in *Devonian of the World*, vol. 2, *Sedimentation*, edited by N. J. McMillan et al., *Mem. Can. Soc. Pet. Geol.*, *14*, 377–392.
Russell, A. D., and J. L. Morford (2001), The behavior of redox-sensitive metals across a laminated-massive-laminated transition in Saanich Inlet, British Columbia, *Mar. Geol.*, *174*, 341–354.
Sageman, B. B., D. J. Hollander, T. W. Lyons, A. E. Murphy, C. A. Ver Straeten, and J. P. Werne (2003), A tale of shales: The relative roles of production, decomposition, and dilution in the accumulation of organic-rich strata, Middle-Upper Devonian, Appalachian Basin, *Chem. Geol.*, *195*, 229–273.
Scranton, M. I., F. L. Sayles, M. P. Bacon, and P. G. Brewer (1987), Temporal changes in the hydrography and chemistry of the Cariaco Trench, *Deep Sea Res., Part A*, *34*, 945–963.
Scranton, M. I., Y. Astor, R. Bohrer, T.-Y. Ho, and F. Müller-Karger (2001), Controls on temporal variability of the geochemistry of the deep Cariaco Basin, *Deep Sea Res., Part I*, *48*, 1605–1625.
Shimkus, K. M., and E. S. Trimonis (1974), Modern sedimentation in Black Sea, in *The Black Sea—Geology, Chemistry, and Biology*, edited by E. T. Degens and D. A. Ross, *AAPG Mem.*, *20*, 249–278.
Shipboard Scientific Party (1997), Site 1002, in *Proc. Ocean Drill. Program Initial Rep.*, *165*, 359–373.
Shipboard Scientific Party (1998), Sites 1033 and 1034, in *Proc. Ocean Drill. Program Initial Rep.*, *169S*, 11–61.
Skei, J. (1981), Et biogeokjemisk studium av en permanent anoksisk fjord—Framvaren ved Farsund (in Norwegian), *Rep. F-80400*, 108 pp., Nor. Inst. for Vannforsk., Oslo.
Skei, J. (1983), Geochemical and sedimentological considerations of a permanently anoxic fjord—Framvaren, south Norway, *Sediment. Geol.*, *36*, 131–145.
Skei, J. (1986), The biogeochemistry of Framvaren: A permanent anoxic fjord near Farsund, south Norway, *Rep. F-80400–I*, 256 pp., Nor. Inst. for Vannforsk., Oslo.
Skei, J. M. (1988), Framvaren—Environmental setting, *Mar. Chem.*, *23*, 209–218.
Skei, J., D. H. Loring, and R. T. T. Rantala (1988), Partitioning and enrichment of trace metals in a sediment core from Framvaren, south Norway, *Mar. Chem.*, *23*, 269–281.
Skei, J., D. H. Loring, and R. T. T. Rantala (1996), Trace metals in suspended particulate matter and in sediment trap material from a permanently anoxic fjord—Framvaren, south Norway, *Aquat. Geochem.*, *2*, 131–147.
Stigebrandt, A., and J. Molvaer (1988), On the water exchange of Framvaren, *Mar. Chem.*, *23*, 219–228.
Taylor, S. R., and S. M. McLennan (1985), *The Continental Crust: Its Composition and Evolution*, 312 pp., Blackwell, Malden, Mass.
Top, Z., and W. B. Clarke (1983), Helium, neon and tritium in the Black Sea, *J. Mar. Res.*, *41*, 1–17.
Top, Z., E. Izdar, M. Ergün, and T. Konuk (1990), Evidence of tectonism from 3He and residence time of helium in the Black Sea, *Eos Trans. AGU*, *71*(32), 1020–1021.

Tugrul, S., O. Basturk, C. Saydam, and A. Yilmaz (1992), Changes in the hydrochemistry of the Black Sea inferred from water density profiles, *Nature*, *359*, 137–139.

Veeh, H. H., S. E. Calvert, and N. B. Price (1974), Accumulation of uranium in sediments and phosphorites of the south west African shelf, *Mar. Chem.*, *2*, 189–202.

Volkov, I. I., and L. S. Fomina (1974), Influence of organic material and processes of sulfide formation on distribution of some trace elements in deep-water sediments of Black Sea, in *The Black Sea—Geology, Chemistry, and Biology*, edited by E. T. Degens and D. A. Ross, *AAPG Mem.*, *20*, 456–476.

Vorlicek, T. P., and G. R. Helz (2002), Catalysis by mineral surfaces: Implications for Mo geochemistry in anoxic environments, *Geochim. Cosmochim. Acta*, *66*, 3679–3692.

Wakeham, S. G. (1990), Algal and bacterial hydrocarbons in particulate matter and interfacial sediment of the Cariaco Trench, *Geochim. Cosmochim. Acta*, *54*, 1325–1336.

Waldron, H. N., and T. A. Probyn (1991), Short-term variability during an anchor station study in the southern Benguela upwelling system: Nitrogen supply to the euphotic zone during a quiescent phase in the upwelling cycle, *Prog. Oceanogr.*, *28*, 153–166.

Wedepohl, K. H. (1971), Environmental influences on the chemical composition of shales and clays, *Phys. Chem. Earth*, *8*, 307–331.

Werne, J. P., D. J. Hollander, T. W. Lyons, and L. C. Peterson (2000), Climate-induced variations in productivity and planktonic ecosystem structure from the Younger Dryas to Holocene in the Cariaco Basin, Venezuela, *Paleoceanography*, *15*, 19–29.

Wignall, P. B. (1994), *Black Shales*, 127 pp., Clarendon, Oxford, UK.

Wilkin, R. T., and M. A. Arthur (2001), Variations in pyrite texture, sulfur isotope composition, and iron systematics in the Black Sea: Evidence for late Pleistocene to Holocene excursions of the O_2-H_2S redox transition, *Geochim. Cosmochim. Acta*, *65*, 1399–1416.

Wilkin, R. T., M. A. Arthur, and W. E. Dean (1997), History of water-column anoxia in the Black Sea indicated by pyrite framboid size distributions, *Earth Planet. Sci. Lett.*, *148*, 517–525.

Wright, J., and A. Colling (1995), *Seawater: Its Composition, Properties and Behaviour*, 2nd ed., 168 pp., Elsevier, New York.

Yao, W., and F. J. Millero (1995), The chemistry of the anoxic waters in the Framvaren Fjord, Norway, *Aquat. Geochem.*, *1*, 53–88.

Yarincik, K. M., R. W. Murray, T. W. Lyons, L. C. Peterson, and G. H. Haug (2000), Oxygenation history of bottom waters in the Cariaco Basin, Venezuela, over the past 578,000 years: Results from redox-sensitive metals (Mo, V, Mn, and Fe), *Paleoceanography*, *15*, 593–604.

Zhang, J.-Z., and J. J. Millero (1993), The chemistry of anoxic waters in the Cariaco Trench, *Deep Sea Res., Part I*, *40*, 1023–1041.

Zheng, Y., R. F. Anderson, A. van Geen, and J. S. Kuwabara (2000), Authigenic molybdenum formation in marine sediments: A linkage to pore water sulfide in the Santa Barbara Basin, *Geochim. Cosmochim. Acta*, *64*, 4165–4178.

T. J. Algeo, Department of Geology, University of Cincinnati, P.O. Box 210013, Cincinnati, OH 45221-0013, USA. (thomas.algeo@uc.edu)

T. W. Lyons, Department of Earth Sciences, University of California, Riverside, Riverside, CA 92521-0423, USA. (timothy.lyons@ucr.edu)